High-throughput Screening of MOF Membranes and MOF/Polymer Mixed Matrix Membranes: Best Materials for Flue Gas Separation

by

Hilal Dağlar

A Thesis Submitted to the

Graduate School of Engineering

in Partial Fulfillment of the Requirements

for the Degree of

Master of Science

In

Chemical and Biological Engineering

Koç University

August 2019

Koç University

Graduate School of Sciences and Engineering

This is to certify that I have examined this copy of a master's thesis by

Hilal Dağlar

and have found that it is complete and satisfactory in all respects,

and that any and all revisions required by the final

examining committee have been made.

Committee Members:

_____

Prof. Seda Keskin Avcı (Advisor, Koç University)

_____

Assoc. Prof. Seda Kızılel (Koç University)

_____

Asst. Prof. İlknur Eruçar Fındıkçı (Özyeğin University)

Date: _____

ABSTRACT

It has become a significant challenge to select the best metal organic frameworks (MOFs) for membrane-based gas separations because the number of synthesized MOFs is growing exceptionally fast. In this thesis, high-throughput computational screening was used to identify the top MOFs used as pure membranes or fillers in polymer membranes for flue gas separation. Firstly, grand canonical Monte Carlo and molecular dynamics simulations were performed to assess adsorption and diffusion properties of CO_2 and N_2 in 3806 different MOFs. Using this data, selectivities and permeabilities of MOF membranes were predicted and compared with those of conventional membranes, polymers and zeolites. The best performing MOF membranes offering CO_2/N_2 selectivity>350 and CO_2 permeability>10^6 Barrer were identified. Ternary $CO_2/N_2/H_2O$ mixture simulations were performed for the top MOFs to unlock their potential under industrial operating conditions and results showed that the presence of water decreases both the CO_2/N_2 selectivity and CO_2 permeability of MOF membranes. Secondly, molecular simulations were also performed to calculate CO_2 and N_2 permeabilities of 7822 synthesized MOFs with the aim of evaluating their performances as fillers in mixed matrix membranes (MMMs). This data was then combined with the experimentally reported gas permeability data of 14 different polymers using a theoretical permeation model. As a result, CO_2 permeabilities and CO_2/N_2 selectivities of 109508 different types of MOF-based MMMs were estimated. The top 50 MOFs that significantly improve CO_2/N_2 separation performances of highly permeable polymers were identified and their potentials for separation of binary CO_2/N_2 mixture were examined at practical operating conditions. Results showed that several MOFs offer significant improvements both in the gas permeability and selectivity of polymers when used as fillers in MMMs for flue gas separation. As a result of this stepwise screening procedure, the number of promising MOFs to be investigated for flue gas separation in future experimental studies was narrowed down from thousands to tens. Throughout the thesis, the MOF structure-membrane performance relations were also investigated to understand which properties of MOFs lead to the greatest promise for flue gas separation.

ÖZET

Membran-temelli gaz ayırımları için en iyi metal organik yapıları (MOF) seçmek önemli bir zorluk haline gelmeye başlamıştır, çünkü sentezlenmiş MOF sayısı olağanüstü bir şekilde artmaktadır. Bu tezde, membran-temelli baca gazı ayırımında membran olarak ya da karışık yataklı membran içerisinde (MMM) dolgu olarak kullanılacak en iyi MOF malzemelerini belirlemek için yüksek çıktılı hesaba dayalı moleküler benzetim yöntemleri kullanılmıştır. Tezin ilk kısmında karbondioksit (CO_2) ve nitrojen (N_2) gazının 3806 MOF'daki adsorpsiyon ve difüzyon özelliklerini değerlendirmek için Grand Canonical Monte Carlo (GCMC) ve Moleküler Dinamik (MD) simülasyonları uygulanmıştır. Bu veri kullanılarak, MOF membranların gaz seçicilikleri ve geçirgenlikleri tahmin edilmiş ve bunlar geleneksel membranlar olan polimerler ve zeolitler ile kıyaslanmıştır. CO_2/N_2 seçiciliği için >350 ve CO_2 geçirgenliği için $>10^6$ Barrer koşulunu sağlayan en yüksek performanslı MOF membranları belirlenmiştir. En iyi MOF'ların potansiyellerini göstermek için bu malzemeler üzerinde üçlü $CO_2/N_2/H_2O$ gaz karışımı simülasyonları uygulanmıştır. Sonuçlar su buharının varlığında hem CO_2/N_2 seçiciliğinin hem de CO_2 geçirgenliğinin düştüğünü göstermektedir. Tezin ikinci kısmında, karışık yataklı membranlarda (MMM) destekleyici bir katman olarak MOF'ların performanslarını değerlendirmek amacıyla 7822 sentezlenmiş MOF'un CO_2 ve N_2gazlarının seçicilik ve geçirgenliği moleküler simülasyonlar aracılığıyla hesaplanmıştır. Bu veri daha sonrasında 14 farklı polimerin deneysel olarak raporlanan gaz geçirgenlikleri ile teorik bir model kullanılarak birleştirilmiştir. Bunun sonucunda 109508 farklı MOF-dolgulu MMM'nin CO_2 geçirgenlikleri ve CO_2/N_2 seçicilikleri hesaplanmıştır. Oldukça geçirgen olan polimerlerin CO_2/N_2 ayırma performansını önemli bir şekilde geliştiren 50 en iyi MOF belirlenmiş ve onların pratik uygulama koşullarında ikili CO_2/N_2 karışımının ayırımındaki performansları incelenmiştir. Sonuçlar birçok metal organik yapının (MOF) baca gazı ayırımı için karışık yataklı membranlarda dolgu olarak kullanıldığı zaman hem gaz geçirgenliğini hem de seçiciliği önemli ölçüde geliştirdiğini gösterilmiştir. Bu çalışma ile, baca gazı ayırımında gelecekte deneysel çalışmalarda incelemek için saf membran olarak ya da MMM'lerde dolgu olarak kullanılabilecek MOF sayısı sayısı binlerden onlara indirilmiştir. Tez boyunca, MOF'ların hani özeliklerinin onları en iyi performansa götürdüğünü anlamak için MOF yapısı ve membran performansı arasındaki ilişki de ayrıca incelenmiştir.

ACKNOWLEDGEMENTS

Foremost, I would like to express my sincere gratitude to my advisor Prof. Seda Keskin for their kind supervision and support. Her guidance helped me in all the time of research and writing of this thesis. It has been a great chance for me to work with her and I am extremely grateful for her assistance and suggestions throughout my study. I want to thank to Assoc. Prof. Seda Kızılel, and Dr. İlknur Erucar Fındıkçı for being my committee members and their valuable time. Financial support provided by the European Research Council (ERC) under the European Union's Horizon 2020 research and innovation programme (ERC-2017-Starting Grant (grant agreement No 756489-COSMOS) is gratefully acknowledged.

One of the biggest chances of my life is to be a member of NEMO. I had unforgettable memoirs in this friendly research group. I would like to also thank Harun Kulak, Gökay Avcı, Vahid Nozari, Ayda Nemati, Özge Kadıoğlu, Muhammad Zeeshan, Saffiye Kavak, Mert Polat, Önder Aksu and Ömer Altundal for their great friendship and support. If you look at thesis of alumni students in NEMO (Nanomaterials, Energy and Molecular Modeling Research Group), you will see that special thanks to Çiğdem Altıntaş are very irreplaceable things. Without any arrogance in any time, she always helps us about academic information, emotional problems and limitless many things. I have inspired from spending her nights in the office, having academic discipline and moral in my master study. I am so grateful to meet such a person, Çiğdem Altıntaş and I desire to continue this friendship throughout my life. I would like to thank İlknur Eruçar and Sadiye Velioğlu for her help, moral support, and being a role model for me. They are really broadening my horizon in my academic career. I also owe special thanks to Ayşenur Değer for spending great times with me in two years. Her friendship was one of the biggest gifts Koç University gave me. I am also very grateful to my best friends, Hasibe Tuncay, Elif Keser, Sühan Artuğ, Elif Akgün and Sevgi Erdoğan for their endless support.

My deepest gratitude goes to my family, Gönül, Muhsin, Ayşenur, Ömer, Sedat and Sevda (sister in law) Dağlar for the support, sympathy, and love they showed me throughout my life. This study could not be completed without their guidance and understanding. Finally, although I know that words cannot express about my feelings and gratitude to his, I also would like to thank my best friend, biggest supporter and husband Yasin Harman for supporting me in every case intellectually and emotionally.

TABLE OF CONTENTS

LIST OF TABLES

LIST OF FIGURES

NOMENCULATURE

CO_2	: Carbon Dioxide	P^{MMM}	: Permeability of MMM
N_2	: Nitrogen	SA	: Accessible surface area
H_2O	: Water	UFF	: Universal force field
MOF	: Metal Organic Framework	QEq	: Charge equilibration method
MMM	: Mixed Matrix Membrane	PIM	: Polymers of intrinsic microporosity
ZIF	: Zeolite Imidazolate Framework	Q_{st}	: Isosteric heat of adsorption (kJ/mol)
IRMOF	: Isoreticular MOF	K	: Henry's constant (mol/kg/Pa)
GCMC	: Grand Canonical Monte Carlo	D	: Self diffusion constant (m^2/s)
EMD	: Equilibrium Molecular Dynamics	U	: Potential Energy
CSD	: Cambridge Structural Database	S_{ads}	: Adsorption selectivity
PTMSP	: Polytrimethylgermylpropyne	S_{diff}	: Diffusion selectivity
PTMGP	: Polytrimethylsilylpropyne	S_{mem}	: Membrane selectivity
DFT	: Density Functional Theory	μ	: Chemical potential (J/mol)
PLD	: Pore limiting diameter (Å)	σ	: LJ distance parameter (Å)
LCD	: Largest cavity diameter (Å)	ρ	: Density (g/cm^3)
ϕ	: Porosity of MOFs	ϕ	: Volume fraction of filler in polymer
P^P	: Permeability of polymer	NVT	: Constant number of molecules, volume and temperature
P^{MOF}	: Permeability of MOF		

Chapter 1: Introduction

Considering the increasing energy demand of our world, it is not possible to entirely stop the use of fossil fuels and resulting anthropological CO_2 emission. As a result of burning of fuels, 41 billion ton of CO_2 has been released to the atmosphere.[1] On the other hand, it is possible to reduce the greenhouse gas emissions by CO_2 capture. There is a tremendous incentive to achieve CO_2 separation from power plant flue gas, which is mostly consists of N_2, with high efficiency. A number of commercial technologies are available for CO_2/N_2 separation including chemical absorption, adsorption, cryogenic distillation and membrane-based separations. Chemical absorption is a widely used process based on the basic principles of mass transfer with a reversible acid-base reaction. In adsorption-based CO_2 separation, gas molecules (adsorbate) contacting with a solid material (adsorbent) basically form chemical or physical bonds with the material and attach to the surface of the material. This process is very significant for gas mixtures, but regeneration cycle of the adsorbent materials is highly important. Cryogenic distillation process needs low temperature meaning that this process consumes large amount of energy. In addition to these commercial technologies, novel methods such as photosynthesis, enzymatic and catalytic routes have been also developed to achieve CO_2 separation using a scalable, cost-effective technology.[2]

Among these technologies, membrane-based CO_2 separation from flue gas, a gas mixture mainly consists of CO_2 and N_2, has been proved to be a potential alternative to the traditional separation methods due to the cost and energy efficient nature of the membranes in addition to their environmentally benign and versatile characteristics.[3] Compared to the other methods for CO_2 separation, membrane based separation process have generally lower operating cost because of not need to be regenerated like absorption

and adsorption CO_2 separation process. In addition to this, membrane-based separation systems have generally simple flowsheet which have no complex control schemes or no mobile equipments excluding pump and condenser. In membrane-based processes, the start-up time required by the process is also considerably shorter than many other processes.[3]

In membrane-based separation process, polymeric membranes have been widely used for CO_2/N_2 separation due to the ease of processability and large-scale production and extensively reviewed in the literature[4-6] in addition to the discussion of the strategies that can improve the construction of more efficient polymeric membranes.[7] Polymeric membranes offer good thermal and mechanical properties for an effective gas separation process even at elevated temperatures but the well-known trade-off between the gas permeability and selectivity of the polymeric membranes has directed the researchers to develop new membrane materials. Polymers having high gas permeabilities generally suffer from low selectivity and polymers offering high selectivity have limited gas permeabilities requiring high surface area-membranes that increase the capital cost of the membrane-based separation process.[8]

Metal organic frameworks (MOFs) are porous structures combining metals with organic linkers.[9] The utmost advantage of MOFs over traditional porous materials is that a very large variety of MOFs having different pore shapes/sizes and chemical functionalities. Thousands of MOFs can be synthesized by changing the combination of metal clusters and organic ligands. MOFs have received significant interest for membrane-based separation process thanks to their interesting physical and chemical properties such as very large surface areas (up to 6000 m^2/g), low densities (0.2-1 g/cm^3) high porosities, a wide range of pore sizes.[10] MOFs are new generation porous materials composed of metal clusters or ions connected by organic ligands to create highly porous frameworks. Due to the large diversity of available metals and ligands, many MOFs with unique physical and chemical properties have been synthesized and reported to date. Large surface areas, high pore volumes, good thermal and mechanical

properties, tunable pore sizes and functionalities of MOFs make them great candidates for gas separation applications.[11-13] Recently, because of the large variety of MOFs, there have been significant efforts on the development of MOF membranes with high stability, high selectivity and high gas permeability in order to achieve efficient CO_2 separations.[14] The variety of MOFs provide an advantage in finding an ideal membrane material compared to the limited number of other nanoporous membranes such as zeolites because tailoring of MOFs for specific applications is easier than zeolites which have rigid and unchanging tetrahedral oxide skeletons to form their pores. The Cambridge Crystallographic Data Centre (CCDC)[15] includes a huge library of MOFs with more than 70,000 entries for synthesized, real MOFs compared to the International Zeolitic Association (IZA) which has 229 zeolitic frameworks. In addition to this, there are many studies to compare adsorption-based CO_2 separation performance of zeolites with those of MOFs and results shows that MOFs are strong alternative to traditional adsorbents.[16]

Mixed matrix membranes (MMMs) combine the processability and mechanical strength of polymers with the good gas separation properties of porous fillers. MMMs are hybrid membranes where the porous fillers are incorporated into the polymer matrix to enhance the permeability and selectivity of the pristine polymer. Early works focusing on zeolite-based MMMs have some practical problems due to the incompatibility between polymer and zeolite but this area has been revitalized by the discovery of MOFs.[17] MOFs have been recently used as filler particles in polymers to make MOF/polymer MMMs showing significantly better gas separation performances than the polymer membranes and some MOF-based MMMs have been presented to exceed the Robeson's upper bound[8] established for polymeric membranes.[18-21] It has been reported that the presence of organic linkers in MOFs enables potentially better interaction with polymers compared to those with zeolites, reducing the non-selective defects at the MOF-polymer interface.[20] It is also important to note that incorporation of MOFs as fillers into polymers is much practical to accelerate the industrialization of MOFs compared to making pure, thin-film MOF membranes since fabrication of MOF-

based MMMs can be envisioned with the minor adaptation of the currently existing membrane technology used for polymers.

Examining MOFs as membranes using purely experimental methods is not straightforward because fabrication and performance tests of a new membrane for a target gas separation require a long time. Therefore, it is not possible to test the performance of every MOF materials for membrane-based CO_2/N_2 separation. Computational studies, especially molecular simulations, provide very useful information for adsorption, diffusion and separation of gases in MOFs.[22] Results of molecular simulations are used to quickly investigate a large number of MOFs to classify a handful of promising materials for a desired separation process. In this way, experiments can be directed to promising materials for accelerating the development of useful MOF membranes. Similar to pure MOF membranes, only a few different types of MOFs such as Cu-BTC, ZIF-8, MIL-53, and UiO-66 were experimentally used in MOF-based MMMs .[23] The large numbers of MOFs create a wide material space to be used as filler particles in the MMMs, however it is also very challenging to select the most appropriate MOF fillers for a given polymer and experimentally fabricate/test the gas separation performances of all possible MOF-based MMMs. Computational studies that can predict the gas separation performances of MOF/polymer MMMs prior to experimental studies play a very important role in identifying the best performing MMMs for a gas separation of interest. On the other hand, there are also time-consuming and more complicated parts in molecular simulations such as collecting diffusion data to compute the performance of membranes and simulating gas mixtures to mimic real conditions. Therefore, computational studies in the literature have been generally focused on adsorption data of single-component gases. For membrane-based gas separation, diffusion data of MOFs is also required, and simulation should be performed to mimic operating conditions of flue gas separation to predict the real potential of MOFs as membranes or filler particles in MMMs.

In this thesis, a high-throughput computational screening method was used to predict the performances of pure MOF membranes and MOF-based MMMs for CO_2/N_2 separation and the best materials were identified. In Chapter 2, a detailed literature review is about MOFs, polymers and MOF/polymer MMMs. In this chapter, experimental and computational studies which have investigated MOF membranes or fillers of MMMs for flue gas separation are given. In Chapter 3, details of molecular simulations used in this study are provided. In Chapter 4, 3806 MOF membranes were examined for CO_2/N_2 separations and the best materials were selected. Humidity effect on the separation performance of membranes was also investigated in this chapter. Chapter 5 demonstrates the performance results of 109508 MOF-based MMMs for CO_2/N_2 separation. In Chapter 4 (5), the relationships between structural properties such as pore sizes, density, porosity, surface area of MOFs and the performance of MOF membranes (MOF-based MMMs) are given. Finally, outcomes obtained from this thesis, challenges and opportunities of high throughput computational screening of MOF membranes and MOF/polymer MMMs are summarized in Chapter 6.

Chapter 2: Literature Review*

In the beginning of this chapter, structural properties, chemical characteristics of MOFs and their related experimental and computational gas separation applications are summarized. In the second part, polymers which are the main materials used as membranes, their limitations and Robeson's upper bound for CO_2/N_2 separation are summarized. Finally, utilization of polymers and MOFs together in different applications is covered and previous works related with MOF/polymer MMMs are discussed.

2.1. Membrane-based Separation by MOFs

MOFs have been considered as novel materials for gas separation process. Gas separation, specifically CO_2 separation using MOFs as adsorbents has been very widely investigated.[24-28] Studies on gas separation with MOF membranes are still limited compared to the adsorption-based separations with MOFs due to the difficulties in fabricating defect-free, thin-film membranes.[29-31] Although several thousands of different MOFs have been deposited to the database, only a very small number of these materials has been fabricated as gas separating membranes.[23] The first attempt was reported by Fischer and co-workers.[32] They modify the crystals of MOF-5 and Cu-BTC to synthesized thin film MOF membrane in 2005. Since then, some of the well-known MOFs such as IRMOF-1 (MOF-5),[33, 34] CuBTC (HKUST-1),[35] ZIF-8 (zeolite imidazolate framework),[36] and ZIF-90[37] have been fabricated and tested as membranes for gas separation applications. These MOF membranes offered high gas

* The literature review about MOF and MOF/Polymer MMM membranes given in this chapter was published in Journal Physical Chemistry C and Advanced Theory & Simulations with following references: Daglar, H..; Keskin, S., *Computational Screening of Metal–Organic Frameworks for Membrane-Based $CO_2/N_2/H_2O$ Separations: Best Materials for Flue Gas Separation.* Journal of Physical Chemistry C. **2018**, *122* (30), 17347–17357.; Daglar, H..; Keskin, S., *High-throughput Screening of MOFs as Fillers in Mixed Matrix Membranes for Flue Gas Separation.* Adv. Theory & Simul., 2019. This chapter is the reformatted version of the mentioned research papers.

selectivities suggesting that they can replace the traditional membrane materials for CO_2 separation processes in the future.[14] In addition to experimental studies of MOF membranes, computational studies provide very useful information for adsorption, diffusion and separation of gases in MOFs.

Similar to experimental studies, in computational screening, several studies have been reported which have used grand canonical Monte Carlo (GCMC) simulations to screen hundreds of different MOF structures in order to identify the best materials for adsorption-based separation of CO_2 from N_2.[38-41] Compared to adsorption-based separation, computational studies of membrane-based gas separation in the literature are still limited. Membrane-based CH_4/N_2 and CO_2/CH_4 separations were examined for MOFs by molecular simulations.[40] Keskin et al. recently examined membrane-based H_2/CH_4 separation performances of MOFs using molecular simulations.[42] However, there is no large-scale molecular simulation study in the literature that screens the entire MOF database for membrane-based CO_2/N_2 separation. One reason is that predicting membrane-based gas separation performances of MOFs requires diffusivities of gas molecules through the membrane material which are obtained from computationally expensive molecular dynamics (MD) simulations of gas mixtures. Adsorption data obtained from GCMC simulations should be combined with the gas diffusion data obtained from MD simulations to estimate permeability and selectivity of the MOF membranes. GCMC and MD simulations of CO_2/N_2 mixture are computationally challenging since they require calculation of the electrostatic interactions between adsorbate-adsorbate (CO_2-CO_2, CO_2-N_2, N_2-N_2) and adsorbate-MOF (CO_2-MOF, N_2-MOF). Both CO_2 and N_2 are polar, multi-atom, linear molecules to non-polar, single atom, spherical representation of H_2 and CH_4. Due to the computational expense and longtime requirement of modeling polar, multi-atom molecules, this type of high throughput molecular simulation study has not been performed for CO_2/N_2 separation. Molecular simulations generally examined a single type of MOF membrane such as IRMOF-1,[43] CuBTC,[44] MgMOF-74,[45] ZnMOF-74,[45] MOF-177,[45] ZIF-8,[46] BioMOF-11[47] for CO_2/N_2 separation. Sumer and Keskin[48] computed CO_2

selectivity and permeability of 5 different MOFs for CO_2/N_2:15/85 mixtures Yilmaz et al.[49] predicted CO_2/N_2 separation performances of 15 different MOFs using molecular simulations. The only study that examined a large number of MOFs for membrane-based CO_2/N_2 separation was performed by Watanabe and Sholl[50] who computed selectivity and permeability of 179 MOF membranes at infinite dilution using GCMC and MD simulations. Their reported CO_2/N_2 selectivity and CO_2 permeability of MOFs were 2-2.6×10^4 and 1-10^8 Barrers, respectively.

2.2. Membrane-based Separation by Polymers

Polymeric membranes have gained importance as the most used materials in gas separation technology because of their easy processability and low cost.[3] Membrane-based gas separation technology was firstly industrialized thanks to asymmetric polymeric and composite membranes used in sea demineralization. These polymeric membranes basically have a composite configuration and they include selective defect-free thin layer and a porous and strong substrate to separate gases from each other.[51] Polymeric membranes have been used for flue gas separation to separate CO_2 from other gases. In membrane-based gas separation, three important criteria are required for good performing polymeric membranes. One is the permeation capacity of the gas through the membrane; second is their ability to separate the gas from other gases and the third criteria is about their thermal and mechanical ability.

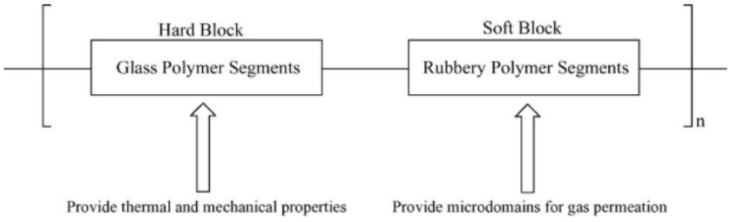

Figure 2.1. Synthetic strategy for polymer structure used as CO_2 separation membranes.[52]

To be clearer, it is explained that the most widely used polymers are constructed with two main parts which are hard block and soft block as shown in Fig.2.1. Hard block is consisted of glassy polymer segments to improve thermal resistance and provide mechanical support. On the other hand, soft block is consisted of rubbery polymer segments to gain flexibility to polymer. Flexible chains make easier the transportation of gas molecules that improve gas permeability. The relationship between hard block and soft block in polymers identifies performance of separation of gas molecules. Thus, polymeric membranes have a trade-off between permeability and selectivity.[52] In the literature, many recent review papers were published on the performance of polymers for flue gas separation.[51] In 2008, Robeson collected the gas separation performance data of many polymeric membranes for CO_2/N_2 separation and derived an upper bound to explain the relationship between selectivity and permeability of CO_2 as shown in Fig. 2.2. Therefore, it is important to exceed the upper bound and solve this trade-off problem between selectivity and permeability to use polymers flue gas separation efficiently.

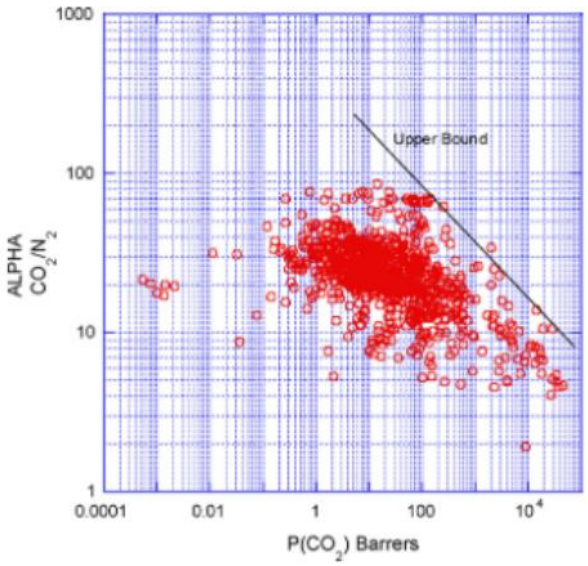

Figure 2.2. Robeson's upper bound for membrane based CO_2/N_2 separation.[8]

2.3. MOF/Polymer Mixed Matrix Membranes (MMMs) for Flue Gas Separation

The difficulties in synthesizing defect-free pure MOF membranes and performance limitations in polymeric membranes have directed the researchers to the combination of MOFs and polymers to make more efficient membrane materials. To improve gas permeability and selectivity together, incorporation of MOFs into polymers has been investigated experimentally and computationally. For example, when Car et al.[53] incorporated two different MOFs (CuBTC and $Mn(HCOO)_2$) as filler particles into two different polymers (polydimethylsiloxane (PDMS) and polysulfone (PSf)), they showed that the CO_2/N_2 selectivity of four MMMs slightly higher than the CO_2/N_2 selectivity of polymeric membranes. Basu et al.[54] measured the mixture gas permeation properties of CuBTC/Matrimid and CuBTC/Matrimid/PSf and they also obtained improvements in both CO_2 permeability and CO_2/N_2 selectivity. Recently, Duan et al. [55]synthesized MMMs incorporated CuBTC into Ultem. Their results showed that using CuBTC as filler particles enhance the CO_2 permeability of Ultem approximately 3 times and whereas do not change the CO_2/N_2 selectivity of the polymer. Kim et al.[56] also used CuBTC to combine with two different polymers (amorphous poly (2-ethly-2 oxazoline and semicrystalline poly(amide-6-b ethylene oxide)). They investigated significant improvement in ideal CO_2 selectivity over N_2 of these polymers. As seen these studies, experimental data on the gas permeability of MOFs is very limited due to the difficulty of these measurements. As a result, almost all the computational screening studies on MOF-based MMMs utilized molecular simulations to estimate the gas permeability of MOFs. This data is then combined with the available experimental gas permeability data of polymers using a theoretical permeation model in order to estimate the gas separation performance of MOF-based MMMs. In the early studies, gas permeabilities of only a small number of selected MOFs have been examined using molecular simulations Yilmaz and Keskin[49] incorporated 15 MOF and 5 ZIF into 16 different polymers to performed CO_2/N_2 separation performance of composed MMMs. They also investigated the effects of flexibility of fillers, loading and operating temperature on the gas separation performance of MMMs. Sumer and Keskin [57] also calculated gas permeability and selectivity of 700 MMMs composed of 70 MOFs and 10 polymers for CO_2/N_2 separation.

Keskin's group also examined the performance of 80 MMMs composed of different MOF and polymers for CO_2/CH_4 separation[58] and several MOF fillers have been shown to improve the gas separation performance of pristine polymers. Lately, with the establishment of computation-ready MOF databases[59, 60] and with the advancement of molecular simulation techniques, high-throughput computational screening of MOFs has been done for different gas separations. High-throughput computational screening is very useful to efficiently identify the most promising MOF/polymer MMMs for target gas separations. For example, Altintas and Keskin[61] applied a multi-level, high-throughput computational screening methodology showing increasing computational expense and complexity at each level to study ~3800 MOFs for CO_2/CH_4 separation. They identified the top 8 MOF fillers from their screening approach and then estimated gas permeabilities and selectivities of MOF-based MMMs composed of these top MOFs and 8 different polymers. Results showed that incorporation of MOFs significantly enhances CO_2 permeabilities of all polymers and even enhances CO_2/CH_4 selectivities of some polymers. Azar et al.[62] used a high-throughput computational screening approach to identify the best MOF fillers for H_2/N_2 separation and presented that incorporating MOFs into polymers almost doubles H_2 permeabilities and some MOFs provide slight enhancements in H_2/N_2 selectivities of polymers. Wilmer et al.[63] computationally screened a large number of real and hypothetical MOFs for CO_2/N_2 separation to predict the cost of carbon capture as a function of selectivity of MOF-based MMMs. They predicted that a large number of MMMs yields a cost of carbon capture <$50 per tonne CO_2 removed. Yan et al.[64] recently performed high-throughput computational screening of covalent organic frameworks (COFs) for CO_2/CH_4 separation and 3 well-performed COFs identified from their computational screening were examined as fillers in MMMs composed of 4 different polymers. Their results showed that some COFs can promote the polymers above the Robeson's upper bound.

As can be seen in this literature review, studies on pure MOF membranes used for CO_2/N_2 membrane separation investigated by permeability and membrane selectivity are

very limited to identify the promising materials. In order to expand the literature about the flue gas membrane-based gas separation, Chapter 4 in this thesis covered computational screening of 3806 MOFs and their membrane-based CO_2/N_2 separation performances. In Chapter 4, the top MOF membranes having high selectivity and high permeability have been selected. These top membranes have been also studied for separation of binary CO_2/N_2 mixtures. However, flue gas includes a small amount of water vapor and this can affect the separation performance of membrane materials. To mimic real operating conditions, humidity effects in flue gas separation have been also investigated as simulating ternary $CO_2/N_2/H_2O$ mixture for top MOF membranes in this computational study. It is shown throughout this thesis that H_2O effect is important for determining the real performances of MOFs for flue gas separation. Results showing important relationships between structural properties of MOF membranes and their gas separation performances are given in Chapter 4.

In the literature review, it is also seen that studies investigating promising MOF/polymer MMMs is limited. Experimental studies use certain types of MOFs and polymers for preparing MOF/polymer MMMs. In addition, there is a limited number of computational studies and only a small fraction of MOFs and polymers was studied. Both experimental and computational studies that are summarized above showed that MOF fillers increase gas permeation . However, to identify the best MOF and polymer pairs offering the best MMMs which have high selectivity and high permeability for CO_2/N_2 separation, it is important to expand the knowledge about new MOF/polymer combinations. Because of impossibility of synthesizing all available MOF/polymer MMMs, large-scale computational screening studies are very important. With this motivation, 7822 real MOFs and 14 polymers leading to 109508 real MMMs were studied in Chapter 5. In addition to this, 200 MOF-based MMMs were studied for CO_2/N_2 mixture separation. This is the largest number of MOF-based MMMs for which synthesized, real MOFs were considered as fillers using high-throughput molecular

simulations. Results of this chapter will help to accelerate the experimental studies aiming to identify MOF and polymer pairs.

Chapter 3: Computational Methods

In this chapter, all computational methods used in this thesis are covered. In the first part, criteria of MOF selection, steps before molecular simulations are described in detail and in the second part, utilization of Grand Canonical Monte Carlo (GCMC) and Molecular Dynamics (MD) simulations to calculate the separation performance of MOFs is summarized. In the last part, calculation of membrane evaluation metrics and theoretical model used for MOF-based MMMs are discussed.

3.1. MOFs and Polymer Selection

Our high-throughput computational screening approach was designed to have increasing complexity and computational cost. In this thesis, two different version of the non-disordered MOF subset of the Cambridge Structural Database (CSD)[60] were used. In Chapter 4, 3806 MOFs having a large variety of chemical and structural properties were studied. These MOFs were taken from the recent collection of MOFs[65] which consists of 54808 non-disordered structures. In Chapter 5, 7822 different types of MOFs representing various structural properties were examined as fillers. These MOFs were taken from the updated version (December 2017) of CSD MOF subset consisting of 70589 MOFs. Except for their version of non-disordered MOF subset of CSD, our elimination procedure of MOF sets used in Chapters 4 and 5 were the same. First, solvent molecules were removed from the pores of these two different set of MOFs using the Python script[60] of the database to imitate the experimental activation procedure of MOFs. Zeo++ software[66] was used to calculate geometrical descriptors of MOFs such as pore limiting diameter (PLD), the largest cavity diameter (LCD), accessible gravimetric surface area (SA), and porosity (ϕ). For surface area calculations number of trials and probe size were set to 2000 and 1.86 Å. In addition, number of trials and probe size of pore volume calculations were set to 50000 and 0 Å, respectively. We only

considered the MOFs with non-zero accessible surface areas. Therefore, refined this large database to only include the MOFs with PLDs >3.75 Å were refined so that both CO_2 (3.3 Å) and N_2 (3.64 Å) molecules can pass through the MOFs' pores.

In Chapter 5, we also used 14 different polymers, Matrimid,[67] Ultem,[68] polyurethane (PU),[69] poly(ether-b-amide) (Pebax),[70] polymethylpentene (PMP),[71] poly(bis(2-(2-methoxyethoxy)ethoxy)phosphazene)(MEEP),[72] 6FDA-2,2-bis(3,4-carboxyphenyl) hexafluoropropanedianhydride-diaminomesitylene (DAM) (6FDA-DAM),[73] 6FDA-2,3,5,6-tetramethyl-1,4-phenylenediamine (6FDA-durene),[74] polymers of intrinsic microporosity-7 (PIM-7),[75] poly(dimethylsiloxane) (PDMS),[76] modified poly(dimethylsiloxane) (modified PDMS),[77] polymers of intrinsic microporosity-1 (PIM-1),[78] poly(trimethylgermylpropyne) (PTMGP),[79] and poly(trimethylsilypropyne) (PTMSP)[79] . Among these polymers, Matrimid, Ultem, PU, Pebax, PMP, PDMS, 6FDA-DAM and 6FDA-durene were studied since they are commonly used in the experimental studies. Additionally, MEEP, PIM-1, PIM-7, modified PDMS, PTMGP and PTMSP were examined since these polymers are close to the Robeson's upper bound established for CO_2/N_2 separation.[8] Single-component CO_2 and N_2 permeabilities of these polymers were collected from the literature and given in Table A.1.

3.2. Molecular Simulations

In this thesis, performances of MOFs for membrane-based gas separation were computed by using two different simulations which are Grand Canonical Monte Carlo (GCMC) and Molecular Dynamics (MD) simulations for single-component gas, binary mixture and ternary mixture data.

3.2.1. Grand Canonical Monte Carlo (GCMC) Simulations

Grand canonical Monte Carlo (GCMC) simulation is commonly used for gas-solid adsorption. In GCMC, chemical potential (μ), volume (V) and temperature (T) are kept constant while the number of molecules (N) are fluctuated to represent experimental conditions considering that chemical potential and temperature of solid adsorbent is the

same with those of outside of the adsorbent. In a GCMC simulation, force field parameters are required for solid materials (MOFs) to calculate energetic interactions including dispersion forces and electrostatic interactions. To represent repulsion and dispersion forces, electrostatic interactions were calculated by using equation of potential energy as follows:

$$U(\mathrm{r}_{ij}) = 4\varepsilon_{ij}\left[\left(\frac{\sigma_{ij}}{r_{ij}}\right)^{12} - \left(\frac{\sigma_{ij}}{r_{ij}}\right)^{6}\right] + \frac{1}{4\pi\varepsilon_0} \times \frac{q_i \times q_j}{r_{ij}} \quad (3.1)$$

This equation is the combination of Lennard Jones potential (LJ 12-6) representing with LJ potential (ε_{ij}) and LJ potential diameter (σ_{ij}) and Coulomb potential representing with the partial charge on atoms (q_i and q_j) and the dielectric constant (ε_0) for energy between two atoms i and j at a distance (r_{ij}). Lorentz-Berhelot mixing rule were used to LJ parameters between dissimilar atoms as:

$$\sigma_{ij} = \frac{\sigma_{ij}+\sigma_{ij}}{2}, \quad \varepsilon_{ij} = \sqrt{(\varepsilon_{ii} \times \varepsilon_{jj})} \quad (3.2)$$

In the literature, there are many force fields directing the accuracy of molecular simulations. Universal force field (UFF)[80] and DREIDING[81] force field are widely used to define potential parameters of MOF atoms in molecular simulations. In this thesis, UFF was used for MOF atoms. Dokur and Keskin[82] showed that although there are significant quantitative differences between some adsorbent evaluation metrics computed using different force fields, rankings of the top MOF materials represented by UFF and DREIDING, separately, for CO_2 separations are generally similar. CO_2 was modeled as a three-site rigid molecule with LJ 12-6 potential and its partial point charges were positioned at the center of each site.[83] N_2 was also represented as a three-site molecule, two sites were located at the N atoms and the third site was located at the center of the mass with partial point charges.[84] and H_2O was represented using the TIP4P[85] model. These values are also shown in Table 3.1

Table 3.1. Parameters used in the modelling of adsorbate molecules.

Gas Molecules	Atoms	σ (Å)	ε/k_B (K)	q (e^-)
CO_2 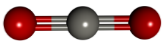	C- CO_2	2.80	27.00	0.70
	O- CO_2	3.05	79.00	-0.35
N_2 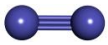	N- N_2	3.31	36.40	-0.40
	COM- N_2	0.0	0.0	0.80
H_2O 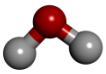	H- H_2O	0.0	0.0	-0.52
	O- H_2O	3.15	77.94	1.04

Since both gas molecules have quadrupole moments, the electrostatic interactions between gas molecules and MOF atoms must be computed. Charge equilibration method (QEq)[86] present in RASPA[87] was used to assign partial point charges to MOF atoms. The electrostatic interactions were calculated by the Ewald summation.[88] The charge assignment method was shown by the good agreements between simulation results and measured CO_2 and N_2 adsorptions of many MOFs using experiments in earlier studies.[41, 48, 89] During GCMC simulations, insertion, deletion, rotation and translation which are four types of moves of molecules were employed to create a new molecule in randomly, delete an existing molecule, rotate an existing molecule randomly and translate a randomly selected molecule, respectively.

In this thesis, molecular simulations for single-component CO_2 and N_2 gases in two different MOF sets were performed. In order to save computational time, molecular simulations of MOFs were initially performed at infinite dilution to compute gas permeabilities. In GCMC, Henry's constants (K^0) of CO_2 and N_2 at infinite dilution, respectively, as implemented in the RASPA simulation code. Henry's constant represents only adsorbent-gas molecule interactions without the presence of gas-gas interactions in infinite dilution. In the second level of calculations in Chapter 4, GCMC simulations were

done for the top 15 MOF membranes considering binary CO_2/N_2:15/85 mixtures at 1 bar and 298 K to represent industrial operating conditions for the flue gas separation. After binary mixture simulations in Chapter 4, we run the molecular simulations for the best MOF membranes identified from the second level of screening for a ternary gas mixture of $CO_2/N_2/H_2O$:10/87/3, which mimics flue gas streams that are usually saturated with water for the industrial post-combustion processes. The partial pressure of water was fixed at 3280 Pa to maintain the relative humidity at 80% whereas the partial pressures of CO_2 and N_2 were set as 9672 and 87048 Pa, respectively to represent the post-combustion process.[90] In Chapter 5, after gas permeabilities of all MOF-based MMMs were estimated at infinite dilution, we aimed to examine mixture separation performance of MOF-based MMMs. We identified the top 50 MOF fillers for highly permeable polymers which lead to the MMMs having the highest CO_2 selectivities. We searched for the available CO_2/N_2 mixture gas permeability data of polymers and obtained this data for 4 polymers, Pebax, 6FDA-DAM, Matrimid and PIM-1 as reported in Table A.2. In order to predict the CO_2/N_2 mixture permeabilities of MOF-based MMMs composed of these polymers, we performed GCMC for the top 50 MOF fillers considering the same gas compositions under the same measurement conditions of these polymers as given in Table A.2. Both adsorbate-adsorbate and adsorbate-MOF interactions were considered for all binary and ternary simulations. A cut-off distance of 13 Å was used to truncate the intermolecular interactions and the simulation cell lengths were increased to minimum 26 Å along each dimension. GCMC simulations were performed for 10000 cycles, the first 5000 for initialization and the last 5000 cycles for getting the ensemble averages.

3.2.2. Equilibrium Molecular Dynamics (EMD) Simulations

Equilibrium Molecular Dynamics (EMD) simulations were performed with the aim of solving the equation of motion of N molecules in three dimensions in a thermodynamically equilibrated system. In this thesis, EMD simulations of adsorbed molecules obtained from GCMC were performed to calculate self-diffusivity of MOFs. Self-diffusivity is the molecular motion of a marked species among other identical

molecules in the fluid.[91] Based on the Einstein's relation, self-diffusion coefficients (D) of gases were computed from the slope of the mean square displacement of gas molecules obtained from EMD simulations. The mean square displacement (MSD) of gas molecules was computed using the equation:

$$MSD(t) = \frac{1}{N}\langle\left(\sum_{j=1}^{N}\left[r_j(t) - r_j(0)\right]\right)^2\rangle \quad (3.3)$$

Here, N is the number of molecules and $r_j\,(t)$ is the three-dimensional position vector of molecule l of species i at time, t. These molecular simulations were performed for 10^6 cycles in the NVT ensemble and a time step of 1 fs was used. The numbers of initialization and equilibration cycles were set as 1000 and 10000, respectively. The Nosé-Hoover thermostat[91] was used in NVT-EMD simulations.

In the first level of EMD simulations, adsorbate-adsorbate interactions were switched-off and 30 adsorbate molecules were inserted into every single MOF to mimic the infinite dilution condition in order to reach a high accuracy in this thesis. We only considered the MOFs in which both CO_2 and N_2 self-diffusivities were calculated to be $>10^{-8}$ cm^2/s, the limit for which diffusion of gases can be readily described using EMD simulations. This restriction eliminates the MOFs for which diffusion selectivity could be very high due to the slow diffusing gas component, but this is necessary to eliminate uncertainties resulting from the time scale limitation of EMD simulations. In chapter 4, for the second level of EMD simulations, the initial states of the mixture EMD simulations were taken from the binary (ternary) GCMC simulations which were carried out for CO_2/N_2:15/85 ($CO_2/N_2/H_2O$:10/87/3) mixtures at 1 bar and 298 K. Minimum 3 trajectories were collected from these simulations to calculate the self-diffusivities of gas molecules. In Chapter 5, mixture EMD simulations were also performed for the top 50 MOF fillers considering the same gas compositions under the same measurement conditions of the polymers as given in Table A.2.

In Chapter 4, both GCMC and EMD simulations were also repeated in the first level of screening by switching-off the electrostatic interactions between guest molecules

and MOFs to investigate their effects on the performance predictions of our molecular simulations. The results of simulations (with and without charges) were compared to elaborate on the necessity of calculating framework charges, which is a computationally time-consuming process in large-scale MOF screening studies. Details are provided in Chapter 4.

3.3. Calculating Membrane Properties of MOFs

K^0 and D^0 values of gases were employed to compute permeabilities of MOFs using the following equation:

$$P_i^0 = K_i^0 \times D_i^0 \tag{3.4}$$

Gas permeabilities were reported in Barrer to be consistent with the literature. Selectivities of the MOF membranes were computed using the ratio of permeabilities of gas species as follows:

$$S^0_{mem,CO_2/N_2} = P^0_{CO_2}/P^0_{N_2} \tag{3.5}$$

Keskin and Sholl [92] estimated that membrane selectivity can be calculated by multiplying adsorption and diffusion selectivities because combination of adsorption and diffusion performances of MOFs represents the performance of membrane-based separation. Adsorption and diffusion selectivities of MOFs were calculated by dividing Henry's constants and self-diffusion coefficients, respectively as follows:

$$S^0_{ads,CO_2/N_2} = K^0_{CO_2}/K^0_{N_2}, \qquad S^0_{diff,CO_2/N_2} = D^0_{CO_2}/D^0_{N_2} \tag{3.6}$$

Both adsorption and diffusion selectivities were computed for CO_2 over N_2 to be consistent with the definition of membrane selectivity.

In the second level of calculations, results of GCMC and MD simulations were used to compute mixture permeabilities in the

$$P_i^{mix} = c_i^{mix} \times D_i^{mix}/f_i \tag{3.7}$$

where c_i, D_i and f_i represent the adsorbed loading of the gas component in the MOF, self-diffusion coefficient of the gas in the mixture and partial pressure of the gas at the feed side of the membrane, respectively. Permeate pressure of the membrane was assumed to be vacuum as validated before.[43] Selectivities of the MOF membranes for gas mixtures were calculated as the ratio of permeabilities of gas species in their corresponding mixtures and referred as 'mixture selectivity' throughout the Chapter 4 as follows:

$$S_{mem}^{mix}=P_{CO_2}^{mix}/P_{N_2}^{mix} \tag{3.8}$$

3.4. Calculating Membrane Properties of MOF/Polymer MMMs

In Chapter 5, since there are two different materials (MOF and polymer) used in equations for MMM, the notations of this chapter are slightly different from those of Chapter 4.

Using the results of molecular simulations, gas permeabilities of MOFs at infinite dilution (P_i^{MOF}) were computed as follows where i represents the gas species:

$$P_i^{MOF}=K_i^0\times D_i^0 \tag{3.9}$$

Selectivities of MOFs (S_{CO_2/N_2}^{MOF}) were computed using the ratio of permeabilities of gas species as follows:

$$S_{CO_2/N_2}^{MOF}=P_{CO_2}^{MOF}/P_{N_2}^{MOF} \tag{3.10}$$

In a previous study, Erucar and Keskin[58] showed that predictions of the modified Felske model has the best agreement with the experiments reporting the CO_2 permeabilities of IRMOF-1/Matrimid MMMs among the theoretical permeation models that consider non-ideal interfacial morphology. Motivated from these results, the modified Felske model was used in this study to estimate the separation performance of all possible MOF-based MMMs for which experimental gas permeability data is not currently available. The modified Felske model predicts the gas permeabilities of MMMs (P^{MMM}) based on the gas permeability of polymer (P^P), permeability of MOF (P^{MOF}),

volume fraction of MOF filler (ϕ) within the polymer matrix and several constants accounting for the interfacial morphology as follows:

$$P^{MMM}=P^{P}\times\left[\frac{1+2\times[(\beta-\gamma)/(\beta+2\gamma)]\times\phi}{1-[(\beta-\gamma)/(\beta+2\gamma)]\times\phi\times\varphi}\right] \quad (3.11)$$

$$\beta=\left(2+\delta^{3}\right)\times\lambda_{mp}-2\times(1-\delta^{3})\times\lambda_{lp},\quad \gamma=\left(1+2\times\delta^{3}\right)-(1-\delta^{3})\times\lambda_{ml},\ \varphi=1+\left[\frac{(1-\phi_{m})}{(\phi_{m})^{2}}\right]\times\phi \quad (3.12)$$

In this model, λ_{mp} is the permeability ratio of P^{MOF}/P^{P}, λ_{lp} is the permeability ratio of P^{I}/P^{P}, P^{I} is the permeability of interphase, P^{P}/β^{*} where the value of β^{*} was taken as 3 following the literature,[93, 94] λ_{ml} is the permeability ratio of P^{MOF}/P^{I}, δ is the ratio of outer radius of the interfacial shell. Parameters used in Eq. (3.12), δ and ϕ_{m}, were taken as 1.18 (obtained for Matrimid/carbon molecular MMM system[95]) and 0.64 (representing the maximum packing volume fraction of the fillers[96]), respectively, from the literature. Furthermore, we also showed that gas permeability predictions of the modified Felske model are in good agreement with the experimentally measured CO_2 and N_2 permeability data for various MOF-based MMMs composed of different MOFs and polymers as discussed in Chapter 5. The volume fraction of MOF fillers in MMMs was used as 0.3 throughout this work following the experimentally fabricated MOF-based MMMs. More details about the usage of this permeation model are available in our previous works.[58, 97] Once the gas permeability of MOF filler computed at infinite dilution as explained above, P^{MOF}, experimentally reported gas permeability of polymer collected from the literature, P^{P}, and the volume fraction of MOF filler, ϕ, were inserted into Eq.(3.11), gas permeability of MMM (P^{MMM}) was calculated. Selectivity of a MOF-based MMM ($S^{MMM}_{CO_2/N_2}$) was calculated as the ratio of gas permeabilities as follows:

$$S^{MMM}_{CO_2/N_2}=P^{MMM}_{CO_2}/P^{MMM}_{N_2} \quad (3.13)$$

Mixture permeabilities of MOF fillers were computed using,

$$P_i^{MOF,\,mix}=c_i^{mix}\times D_i^{mix}/f_i \quad (3.14)$$

where c_i, D_i, and f_i correspond to the adsorbed gas loading of species i computed from GCMC simulations, self-diffusion coefficient of gas species i computed from MD simulations and feed side partial pressure of the gas species i, respectively. Selectivities of MOF fillers at the binary mixture conditions were computed as the ratio of gas permeabilities as follows:

$$S_{CO_2/N_2}^{MOF,\,mix} = P_{CO_2}^{MOF,\,mix} / P_{N_2}^{MOF,\,mix} \tag{3.15}$$

Once the mixture gas permeability of MOF filler, $P_i^{MOF,\,mix}$, experimentally reported gas permeability of polymer collected from the literature, $P^{P,mix}$, and the volume fraction of MOF filler, ϕ, were inserted into Eq.(3.11), mixture gas permeability of MMM ($P^{MMM,\,mix}$) was calculated. Mixture selectivity of a MOF-based MMM ($S_{CO_2/N_2}^{MMM,\,mix}$) was calculated as the ratio of mixture permeabilities as follows:

$$S_{CO_2/N_2}^{MMM,\,mix} = P_{CO_2}^{MMM,\,mix} / P_{N_2}^{MMM,\,mix} \tag{3.16}$$

Chapter 4: Computational Screening of MOFs for Membrane-based $CO_2/N_2/H_2O$ Separations: Best Materials for Flue Gas Separation[†]

In this chapter, we screened the most complete and recent MOF database[60] maintained by the Cambridge Structural Database (CSD)[98] to find out the best membrane materials for CO_2/N_2 separation. This recent MOF database has not been investigated for any membrane-based CO_2 separation application to date. A high-throughput computational screening approach of increasing complexity and computational cost was used: First, GCMC and MD simulations were performed to acquire adsorption and diffusion data of CO_2 and N_2 in all MOFs at infinite dilution condition. Using this adsorption and diffusion data, MOF membranes' selectivity and gas permeability were estimated. Predicted CO_2/N_2 selectivities and CO_2 permeabilities of 3806 MOFs were compared with those of widely studied polymers and zeolites. Promising MOF membranes that can exceed the upper bound[8] were identified. We also repeated both the GCMC and MD simulations by switching-off the gas-MOF electrostatic interactions to reveal the influence of these interactions on the predicted performance of MOF membranes. GCMC and MD simulations of CO_2/N_2:15/85 mixtures were then carried out for the top 15 MOF materials to evaluate their flue gas separation performances under practical conditions, 1 bar and 298 K. Finally, molecular simulations were performed for ternary $CO_2/N_2/H_2O$:10/87/3 mixtures to investigate the effect of presence of water in the flue gas streams on the selectivity and permeability of the top MOF membranes. By applying this stepwise screening procedure, the number of promising MOF membranes for flue gas separation was narrowed down from thousands to tens. Structural properties of MOFs were examined to gain molecular-level insights

[†] The results given in this chapter were published in Journal of Physical Chemistry C with following reference: Daglar, H..; Keskin, S., *Computational Screening of Metal–Organic Frameworks for Membrane-Based $CO_2/N_2/H_2O$ Separations: Best Materials for Flue Gas Separation.* J. Phys. Chem. C, **2018**, *122* (30), 17347–17357. This chapter is the reformatted version of the mentioned research paper.

about the influence of physical and chemical belongings of materials on the membranes' performances. The quantitative structure-performance relationships provided will be used as a guide to direct the design of new MOF membranes having extraordinarily good performances for flue gas separation. The structural properties and the results of gas separation performance of 3806 MOFs in this chapter are given in a publicly accessible database (https://cosmoserc.ku.edu.tr/).

4.1. Screening of MOF Membranes

Before analyzing the results of the computational screening of MOF membranes, predictions of our molecular simulations with available experimental data for CO_2 and N_2 permeabilities of different MOF membranes were compared in Figure 4.1. Conditions of the molecular simulations were same with the experiments. Details of these conditions together with the experimental membrane references are available in Table A.3. Figure 4.1 shows that there is a remarkably good agreement between our molecular simulations and experimental measurements for single-component CO_2 and N_2 permeabilities of IRMOF-1, MIL-53 (Al), Ni-MOF-74, ZIF-90 and ZIF-95 membranes in addition to the CO_2/N_2 mixture permeabilities reported for ZIF-69 membrane.

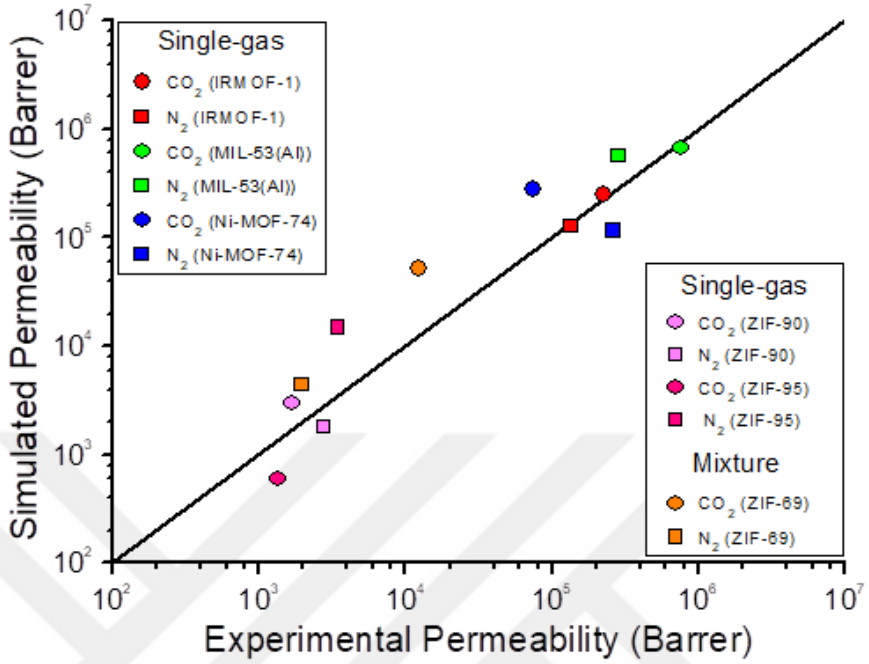

Figure 4.1. Comparison of our simulated gas permeabilities with the experimental data for various MOF membranes. Measurement conditions and related experimental references are given in Table A.3.

Molecular simulations generally overestimate the gas permeabilities compared to the experiments due to the perfect, defect-free membrane assumption, which may not be true in experiments. The good agreement shown in Figure 4.1 demonstrated validity of our computational method. Motivated from this, we used the same method to study 3806 MOFs for membrane-based CO_2/N_2 separation with the aim of identifying the best membrane candidates.

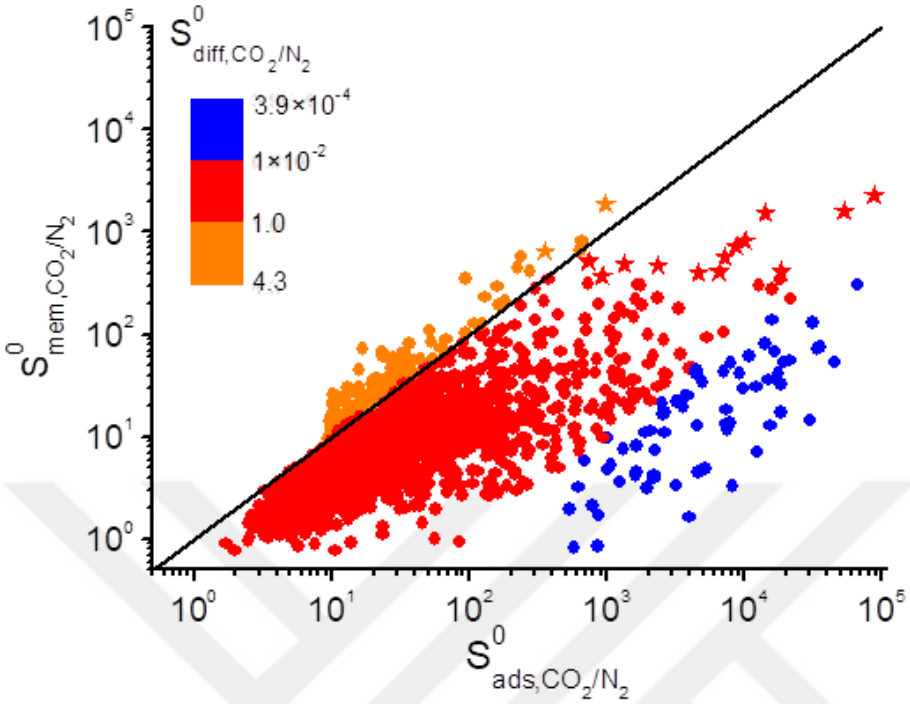

Figure 4.2. Adsorption, diffusion and membrane selectivities of 3806 MOFs for CO_2/N_2 separation computed at infinite dilution at 298 K. Stars represent the top 15 MOF membranes.

Adsorption, diffusion and membrane selectivities of MOFs computed at infinite dilution were shown in Figure 4.2 to assess the impact of adsorption and diffusion of gases on the membrane performance. All selectivities were calculated using the equations described in Chapter 3. Adsorption selectivities of all MOFs favor CO_2 over N_2 since CO_2 is more strongly adsorbed than N_2 and they are between 1.72 and 8.8×10^4. To be consistent with the adsorption selectivity, both diffusion and membrane selectivities are given for CO_2 over N_2 in Figure 4.2. Diffusion selectivities for CO_2/N_2 range from 3.94×10^{-4} to 4.31. In a very large number of MOFs (3664) shown by red and blue points, diffusion selectivities are less than 1 since CO_2 diffuses slower than N_2. In 65 MOFs, N_2 diffusion is significantly faster than that of CO_2 resulting in diffusion selectivities

between 3.9×10^{-4}-0.01 as shown by blue points. In 142 MOFs, CO_2 diffuses faster than N_2 and diffusion selectivities become larger than 1, represented by orange points in Figure 4.2. In fact, those points represent the MOF membranes in which both adsorption and diffusion favor CO_2 over N_2. Membrane selectivities of MOFs computed at infinite dilution ($S^0_{mem,\ CO_2/N_2}$) were between 0.76-2288. Almost all the MOFs (3795) were identified to be CO_2 selective membranes for flue gas separation. Only 11 MOFs have membrane selectivities less than 1 (0.76-1) indicating that they are very weakly N_2 selective. MOFs combining high adsorption selectivity towards CO_2 with low diffusion selectivity towards N_2 become the top promising membranes and stars in Figure 4.2 represent the best membrane candidates, as it is discussed in detail below.

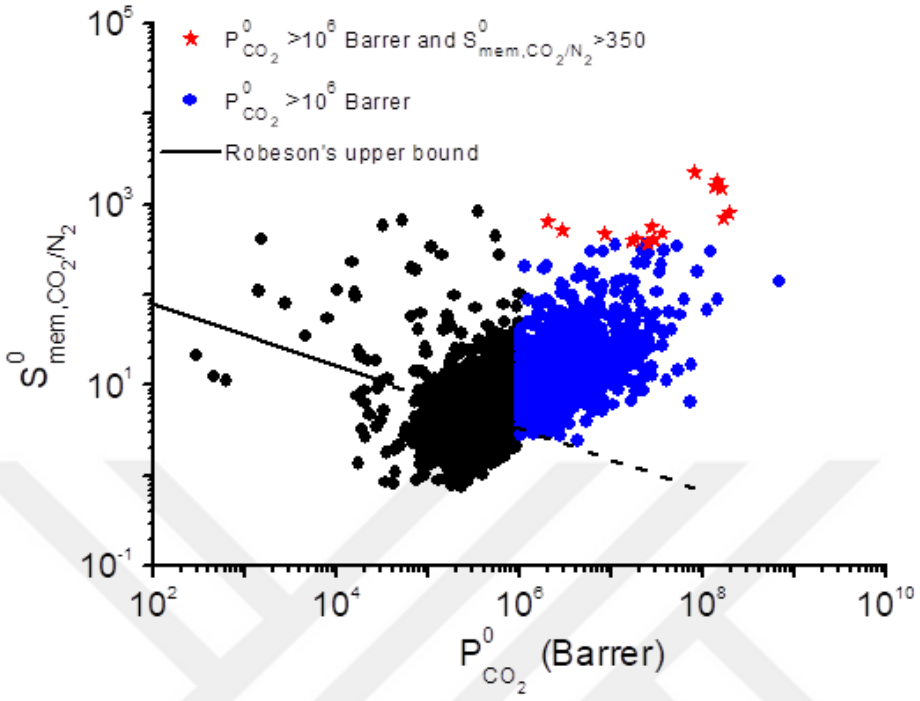

Figure 4.3. Predicted CO_2/N_2 selectivity and CO_2 permeability of 3806 MOF membranes at infinite dilution at 298 K. Red stars represent the best membrane candidates.

Figure 4.3 shows our predictions for CO_2/N_2 selectivities and CO_2 permeabilities of MOF membranes. Polymer membranes have been widely used for CO_2/N_2 separation and Robeson[99] defined the upper bound for the separation performances of polymers as shown with a line in Figure 4.3. The CO_2 permeabilities of MOF membranes were calculated to be considerably larger than those of polymers, ranging from 296 to 6.72×10^8 Barrer since MOFs are highly porous structures compared to polymers. Therefore, we extended the upper bound in Figure 4.3. A significant number of MOFs (2922), almost 77%, were found to surpass the upper bound due to their very high CO_2 permeabilities, $>10^6$ Barrer, as shown by blue points. Highly permeable membranes are strongly desired because they require low surface area, hence low capital cost for the membrane-based gas separation process. Figure 4.3 indicates that many MOF membranes may replace

conventional polymer membranes. We specifically focused on the MOFs that have $S^0_{mem,\ CO_2/N_2}$>350 and $P^0_{CO_2}$>10^6 Barrer to identify the promising membranes having high CO_2/N_2 selectivities and high CO_2 permeabilities. The red stars in Figure 4.3 represent the top 15 MOF membrane candidates that satisfy those two criteria. For these MOFs, binary CO_2/N_2 and ternary $CO_2/N_2/H_2O$ mixture simulations were performed to assess their potentials under industrial operating conditions and results are discussed in the section 4.2.

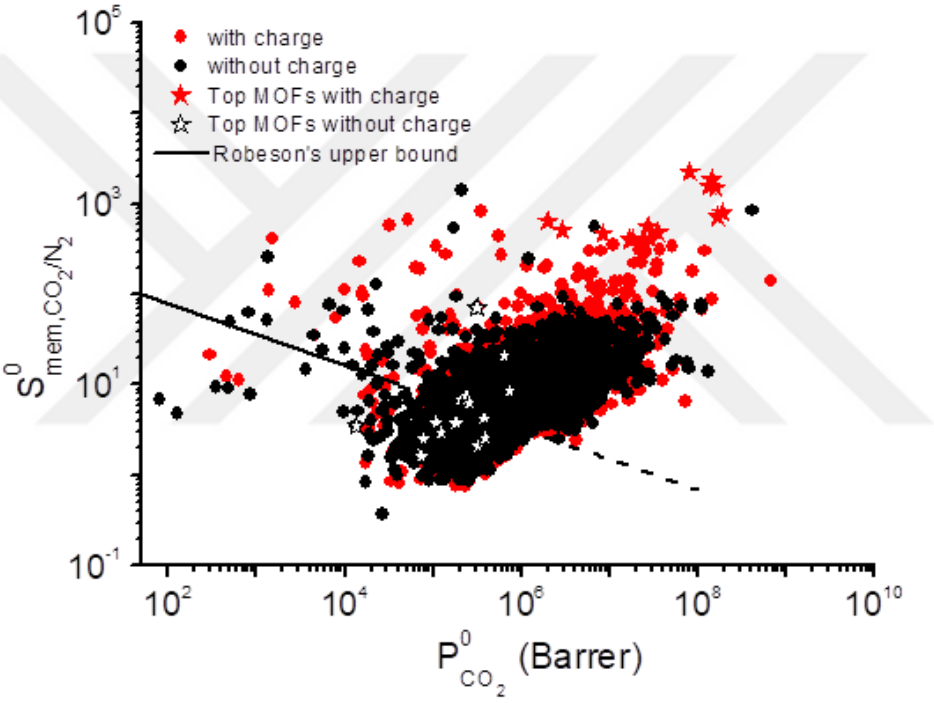

Figure 4.4. Comparison of CO_2/N_2 selectivity and CO_2 permeability of MOF membranes computed with and without framework charges at infinite dilution at 298 K. Red and black stars represent the best membrane candidates computed with and without charges.

As we discussed in the beginning, one challenge of studying adsorption and diffusion of CO_2 and N_2 molecules in MOFs is calculating the electrostatic interactions

between gases and framework atoms which requires computation of partial point charges for MOF atoms. This is a time-consuming process considering the facts that some MOFs have very large structures with several thousands of atoms and there are already thousands of MOFs that we aim to study. In order to understand the effects of electrostatic interactions between the adsorbate molecules and frameworks on the membranes' performances, we repeated all molecular simulations by switching-off the gas-MOF electrostatic interactions. Our aim at that point was to examine whether screening MOF membranes for separation of two polar molecules (CO_2/N_2) can be done by skipping the tedious charge assignment procedure to save significant computational time. Figure 4.4 compares CO_2/N_2 selectivities and CO_2 permeabilities of MOF membranes calculated from molecular simulations considering electrostatic interactions (referred as with charges) with the ones computed by neglecting these interactions (refereed as without charges). The range of calculated CO_2 permeabilities decreased from 296-6.72×10^8 Barrer to 81-4.18×10^8 Barrer when the framework charges were neglected. Similarly, the range of predicted CO_2/N_2 selectivities changed from 0.76-2288 to 0.37-1405. As can be seen from Figure 4.4, the top 15 MOFs that we identified would have been missed if the electrostatic interactions between gas molecules and MOFs were neglected. In fact, most of the promising MOF membranes were located under the upper bound when framework charges were absent.

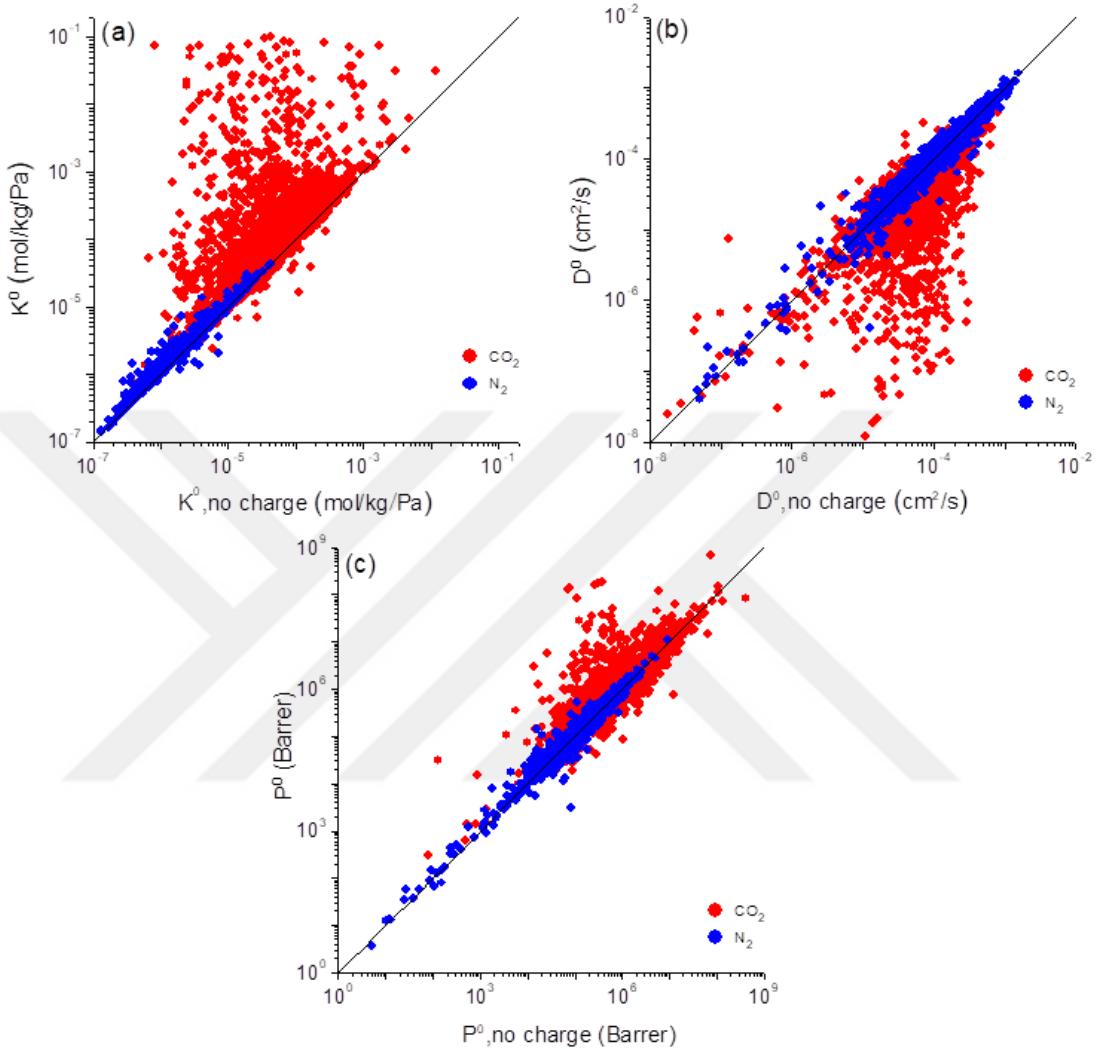

Figure 4.5. Comparisons of (a) Henry's constants (b) self-diffusivities(c) permeabilities of gases computed with and without charges at infinite dilution at 298 K.

Effects of the electrostatic interactions on the gas adsorption and diffusion in MOFs were studied in detail. Figure 4.5(a) represents the Henry's constants (K^0) of CO_2 and N_2 in MOFs computed with and without charges. K^0 values of CO_2 are larger than those of N_2 supporting the fact that MOFs are CO_2 selective in adsorption. Comparison of K^0

values calculated with and without charges showed that neglecting charges significantly underestimates the $K^0_{CO_2}$ in many MOFs whereas the effects of charges is less pronounced for $K^0_{N_2}$ due to the slighter quadrupole moment of N_2 (4.7 cm^2) compared to CO_2 (13.4 cm^2).[100] Figure A.1(a) represents adsorption selectivities of MOFs calculated at infinite dilution as the ratio of Henry's coefficients of gases and neglecting charges resulted in lower CO_2/N_2 adsorption selectivities since $K^0_{CO_2}$ was underpredicted. There are many MOFs for which adsorption selectivity significantly decreased from thousands to tens in the absence of framework charges. Effect of framework charges on the self-diffusion coefficients (D^0) of gases is shown in Figure 4.5(b). $D^0_{CO_2}$ ($D^0_{N_2}$) values vary between 1.21×10^{-8}-6.19×10^{-4} (3.95×10^{-8}-1.61×10^{-3}) cm^2/s. Simulations without MOF charges overpredicted CO_2 diffusivities because CO_2 molecules are less strongly adsorbed in MOFs in the absence of electrostatic interactions and therefore they diffuse faster. The effects of charges on N_2 diffusivities were insignificant. As a result of this, CO_2/N_2 diffusion selectivities were overpredicted when the electrostatic interactions were switched-off as shown in Figure A.1(b). Neglecting MOF charges decreased the adsorption of CO_2 but increased the diffusion of CO_2. The decrease in CO_2 permeability in the absence of charges shown in Figure 4.5(c) indicates that adsorption is the dominant factor in determining CO_2 permeability of membranes. Overall, switching-off the electrostatic interactions between gas-MOF underestimates both CO_2 permeabilities and CO_2 selectivities whereas N_2 permeabilities are almost unchanged. There are significant differences between the CO_2 permeability predictions of simulations considering MOFs' charges and the ones neglecting charges as shown in Figure 4.4. On the other hand, correlation between the rankings of MOFs in terms of CO_2 separation performances obtained from those two sets of simulations is good. We computed the Spearman's ranking correlation coefficient ($-1\leq SRCC\leq 1$) for the MOFs ranking obtained from simulations with and without charges. The SRCC for the rankings of MOFs in terms of CO_2 permeability (CO_2/N_2 selectivity) obtained from simulations with and without charges was calculated to be 0.85 (0.77). These results indicate that neglecting the gas-

MOF electrostatic interactions may be a reasonable approximation in quickly ranking MOF membranes in terms of CO_2 permeabilities and selectivities. This would save tremendous amount of time since assigning partial charges to thousands of MOFs is computationally costly even if approximate methods are used. On the other hand, caution should be warranted because neglecting charges does not accurately identify the most promising MOF membranes as shown in Figure 4.4.

4.2. Binary and Ternary Mixture Separations

All the membrane properties of MOFs discussed above were calculated using single-component adsorption and diffusion data of gases at infinite dilution. It is discussed that multi-component mixture effects could impact the membrane selectivities.[101, 102] However, performing computationally demanding MD simulations for several thousands of MOF membranes is not trivial. Considering the fact that MOF membranes with low ideal membrane selectivities are unlikely to exhibit high mixture selectivity at practical operating conditions, we performed GCMC and MD simulations for binary CO_2/N_2:15/85 mixtures only for the top 15 MOF membranes which were identified in the first-level of screening based on the criteria of $S^0_{mem,\ CO_2/N_2}$>350 and $P^0_{CO_2}$>10^6 Barrer. Mixture simulations were done at 1 bar and 298 K to represent post-combustion CO_2 capture conditions. Table 4.1 summarizes separation performances of the top 15 MOF membranes for binary CO_2/N_2 mixture. Mixture selectivities of MOF membranes were estimated to be high, 16.4-819. Nine of the top 15 MOFs have CO_2/N_2 selectivities>100. CO_2 permeabilities of these MOFs were also calculated to be high, 1.19×10^5-1.95×10^6 Barrer. One common feature of top MOFs is that they all have high adsorption selectivities, generally >100.

Table 4.1. Predicted CO_2/N_2 mixture separation performances of the top 15 MOFs. MOFs are ranked based on their membrane selectivities.

MOF	PLD, LCD (Å)	$D^{mix}_{CO_2}$ (cm^2/s)	$D^{mix}_{N_2}$ (cm^2/s)	$P^{mix}_{CO_2}$ (Barrer)	$P^{mix}_{N_2}$ (Barrer)	$S^{mix}_{ads,\ CO_2/N_2}$	$S^{mix}_{diff,\ CO_2/N_2}$	$S^{mix}_{mem,\ CO_2/N_2}$
VIHHIE	4.55, 6.17	8.48×10^{-6}	2.33×10^{-5}	1.87×10^{6}	2.28×10^{3}	2251.99	0.36	819.86
LUPQES	4.03, 4.70	8.18×10^{-7}	2.69×10^{-6}	1.19×10^{5}	1.75×10^{2}	2234.37	0.30	680.99
AFEJEA	3.77, 4.56	3.64×10^{-6}	4.60×10^{-6}	2.72×10^{5}	6.06×10^{2}	567.36	0.79	449.33
NURVAZ	6.00, 6.58	5.80×10^{-6}	2.33×10^{-5}	9.35×10^{5}	3.04×10^{3}	1238.62	0.25	307.77
PEXSAO	4.26, 5.95	5.41×10^{-6}	2.03×10^{-6}	3.56×10^{5}	1.23×10^{3}	108.25	2.66	288.45
SAJFEO	6.00, 6.63	5.67×10^{-6}	2.51×10^{-5}	9.16×10^{5}	3.26×10^{3}	1245.93	0.23	280.89
PEXROB	4.29, 5.91	5.95×10^{-6}	2.92×10^{-6}	3.94×10^{5}	1.65×10^{3}	117.46	2.04	239.15
LIFWON	3.91, 5.03	1.97×10^{-5}	5.41×10^{-5}	1.95×10^{6}	1.07×10^{4}	499.68	0.36	182.30
PEXSES	4.25, 5.93	2.03×10^{-6}	2.45×10^{-6}	1.81×10^{5}	1.09×10^{3}	200.67	0.83	165.80
ICORAV	4.39, 4.98	2.04×10^{-6}	2.69×10^{-5}	2.07×10^{5}	4.76×10^{3}	574.94	0.08	43.57
KIPJUQ	6.98, 7.29	2.49×10^{-6}	5.71×10^{-5}	1.82×10^{5}	6.24×10^{3}	670.43	0.04	29.21
OGALOZ	3.80, 6.36	8.24×10^{-6}	4.22×10^{-5}	4.93×10^{5}	2.31×10^{4}	109.01	0.20	21.28
OGAHOV	3.83, 6.27	8.85×10^{-6}	4.05×10^{-5}	5.01×10^{5}	2.50×10^{4}	91.97	0.22	20.08
OGAMOA	3.80, 6.37	9.36×10^{-6}	5.11×10^{-5}	5.36×10^{5}	2.99×10^{4}	97.83	0.18	17.91
OGALIT	3.84, 6.37	7.67×10^{-6}	4.78×10^{-5}	4.40×10^{5}	2.69×10^{4}	102.27	0.16	16.38

According to Table 4.1, VIHHIE is the most promising membrane candidate with the highest selectivity, 820. This high membrane selectivity can be explained with the very high adsorption selectivity of this MOF for CO_2 over N_2, 2252. Table 4.1 illustrates that top MOFs, including VIHHIE, are generally the ones having narrow pores. PLDs and LCDs of the top MOFs are between 3.77-6.98 Å and 4.51-7.29 Å, respectively. MOFs possessing small pores offer high CO_2/N_2 adsorption selectivity because of the strong confinement of the adsorbate molecules as demonstrated in Figure A.2(a). Strongly adsorbed CO_2 molecules diffuse slower than the weakly adsorbed N_2 in the narrow pores and diffusion selectivity favors N_2 in all top MOFs except two, also supported by Figure A.2(b). As a result, high adsorption selectivity towards CO_2 dominates the diffusion selectivity towards N_2 in these narrow-pored type materials, leading to high membrane selectivities as shown in Figure A.2(c). Figure A.2(a) also shows that MOFs with large pore sizes (>15 Å) and high porosities generally have low adsorption selectivities. Both

gas molecules diffuse in similar rates in large pores and CO_2/N_2 diffusion selectivities become unity in these MOFs as shown in Figure A.2(b). As a result, membrane-based separation potential of the large-pored MOFs becomes low as shown in Figure A.2(c) and these MOFs are absent in the top material list.

We also compared selectivities and permeabilities of the top MOF membranes with zeolite membranes. Kusakabe et al.[103] reported the CO_2/N_2 selectivity of NaY zeolite membrane as 20 and its CO_2 permeance was measured as 1.6×10^{-7} mol/($m^2\times s\times Pa$) (corresponding to 9.5×10^3 Barrer) at 303 K for a CO_2/N_2:50/50 mixture. Selectivity of ZSM-5 membrane was reported to be 68 for an equimolar mixture at room temperature.[104] Li and Fan[105] used SAPO-34 membranes and reported CO_2/N_2 selectivity in the range of 21-32 and CO_2 permeance of 1.5×10^{-6} mol/($m^2\times s\times Pa$) (corresponding to 2.2×10^4 Barrer) for an equimolar mixture. Molecular simulations of Krishna and van Baten[45] for CO_2/N_2:15/85 mixture at 10 bar and 300 K showed that several zeolites such as FAU, MFI, DDR, and CHA membranes exceed the upper bound with CO_2/N_2 selectivities of 7, 10, 20, 40, respectively. These results showed that top MOF membranes given in Table 4.1 have higher selectivities and permeabilities than zeolite membranes under similar conditions. Results of our molecular simulations for MOFs were also compared with the previous simulation works on MOF membranes. CO_2/N_2 selectivities of Mg-MOF-74, Zn-MOF-74, and MOF-177 were computed as 18, 6, and 2, respectively considering CO_2/N_2:15/85 mixture at 1 bar and 300 K.[45] Our computed CO_2/N_2 selectivities for these MOFs, 12, 5, and 1, agreed well with the literature. We calculated CO_2/N_2 selectivity of ZIF-8 as 5.2, in a good agreement with the previously computed value of 5.7 at infinite dilution.[46] Li et al.[47] computed CO_2/N_2 selectivity of bio-MOF-11 membrane as 22 for CO_2/N_2:15/85 mixture at 1 bar and 298 K. This value is close to the selectivity computed in this work, 18. Watanabe and Sholl[50] predicted CO_2/N_2 selectivities of 179 MOF membranes in the range of 2-2.6×10^4 at infinite dilution. Selectivity of the MOFs we studied in this work is lower than theirs because they only considered MOFs with very narrow pores, 2.2<PLD<3.6 Å, to

study molecular sieve effects of MOF membranes whereas the lowest pore size in our MOF database was 3.75 Å to let both gas molecules to diffuse through the pores.

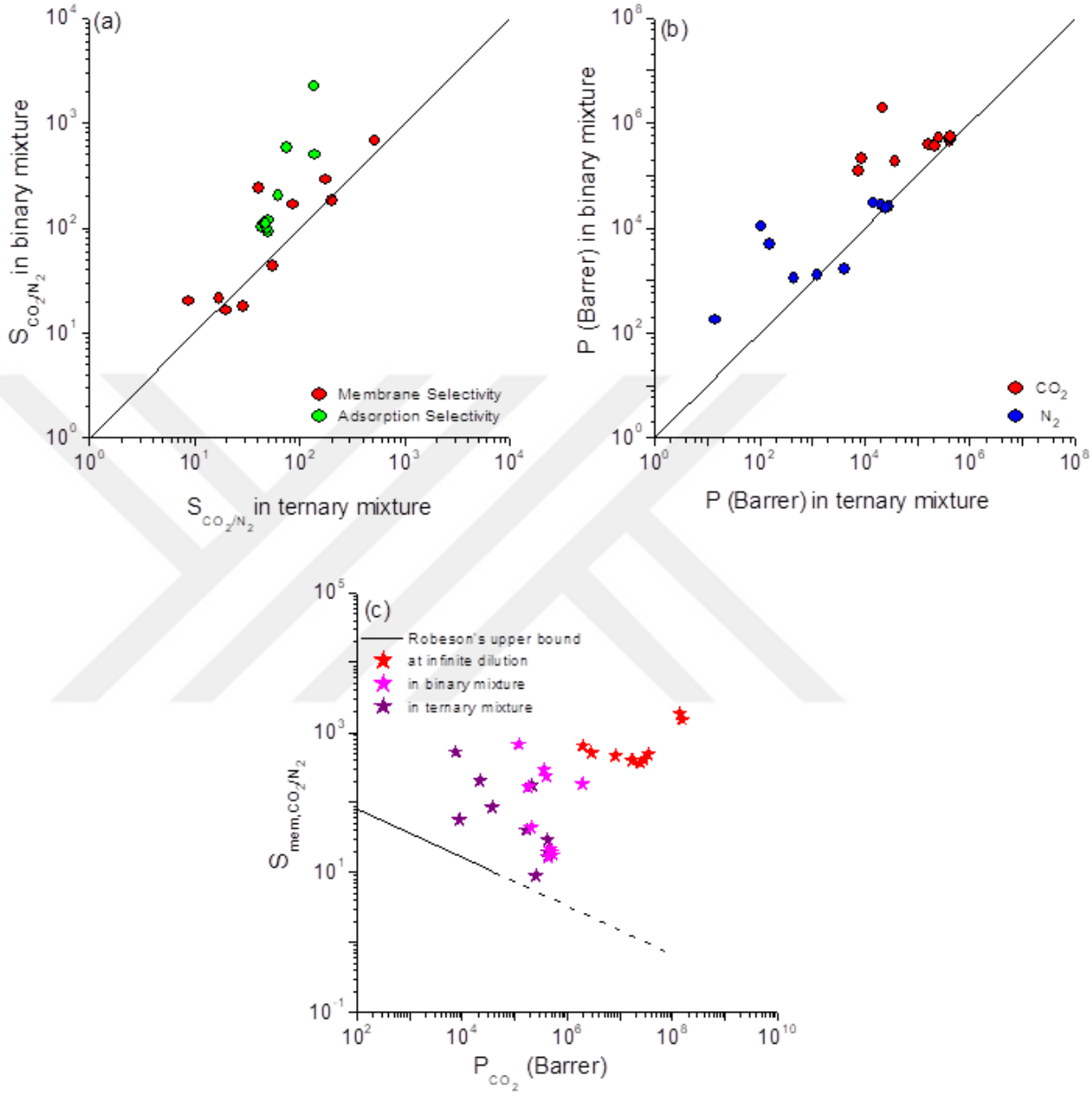

Figure 4.6. Comparison of (a) adsorption and membrane selectivities, (b) gas permeabilities calculated for binary CO_2/N_2 mixture and ternary $CO_2/N_2/H_2O$ mixtures. (c) Comparison of separation performances of the top MOF membranes computed using single-component gas, binary gas mixture and ternary gas mixture simulations.

We finally examined the influence of humidity on the flue gas separation performances of the top MOF membranes using molecular simulations. A ternary gas mixture of $CO_2/N_2/H_2O$:10/87/3 was considered to mimic flue gas streams for the industrial post-combustion processes. It is important to note that ternary MD simulations were performed only for 10 of the top MOFs due to the difficulty of equilibration of highly polar H_2O molecules in the MOFs during GCMC and MD simulations. GCMC simulations showed that H_2O molecules adsorb in MOFs and compete with the strongly adsorbed CO_2 molecules rather than the weakly adsorbed N_2 molecules. The amount of adsorbed CO_2 decreases in the presence of H_2O in agreement with the literature[41, 106, 107] whereas N_2 adsorption is not significantly affected. Therefore, CO_2/N_2 adsorption selectivities computed for ternary mixtures were found to be less than those calculated for binary mixtures in Figure 4.6(a). Diffusivities of gases do not significantly differ in the binary and ternary mixtures. Consequently, permeabilities and membrane selectivities of MOFs computed mimicking the presence of humidity were found to be generally less than those computed for binary mixture as shown in Figure 4.6(b). There are significant decreases in the gas permeabilities of 3 MOFs when a ternary gas mixture was considered. A detailed analysis on these materials showed that these 3 MOFs have the narrowest pore sizes among the top MOFs. Therefore, the reduction in their CO_2/N_2 adsorption selectivities was more distinct than the others, resulting in more observable reductions in their gas permeabilities. Figure 4.6(c) compares the selectivities and permeabilities of the top MOF membranes computed from different levels of our screening approach, using single-component gas data, binary mixture data and ternary mixture data. The top MOF membranes identified at the first level of screening (infinite dilution) are above the upper bound at the more detailed steps of the screening when binary and ternary mixture simulations were performed. These results indicate that screening MOFs in terms of membrane selectivity and permeability considering single-component gases or binary flue gas mixture works well for accurately identifying the best performing MOF membranes for separation of humid flue gas mixture. Finally, we would like to note that our molecular simulations did not give any information about the stability

of MOF membranes under water vapor. Some MOFs are known to lose their crystal structures under humid atmospheric conditions.[108] This type of membranes may not be useful although they possess very high CO_2 selectivities. This issue is more likely to be examined by further experimental studies on the top materials.

4.3 Structure-Performance Relationship of MOF Membranes

One of the advantages of studying a large material database is to get insight on the structure-performance relationships. If clear relationships can be established between structural descriptors of MOFs (size of the pore openings, pore volume, surface area) and their membrane performance such as selectivity, one can easily estimate flue gas separation performance of a newly synthesized MOF by just examining its structural properties. If these relations also include direct structural information such as metal type and lattice type of the MOFs, it can facilitate experimental studies to make MOFs with the appropriate structural properties that can lead to materials having high separation performance. With this motivation, we investigated the distribution of PLD, LCD, ϕ, SA, ρ, metal type and Bravais lattice on all MOFs and on the top 15 MOFs. Figure 4.7 shows that 35 (54) % of all MOFs and 73 (53) % of the top 15 membranes have PLDs<4.5 Å (6<LCD<12 Å). None of the top MOF membranes have pore sizes >12 Å. 80% of the top MOFs have porosities between 0.5 and 0.75. Half of the MOFs we considered and 80% of the top membranes were found to have SA<1000 m^2/g. MOFs with large SA>2000 m^2/g are not top membrane candidates.

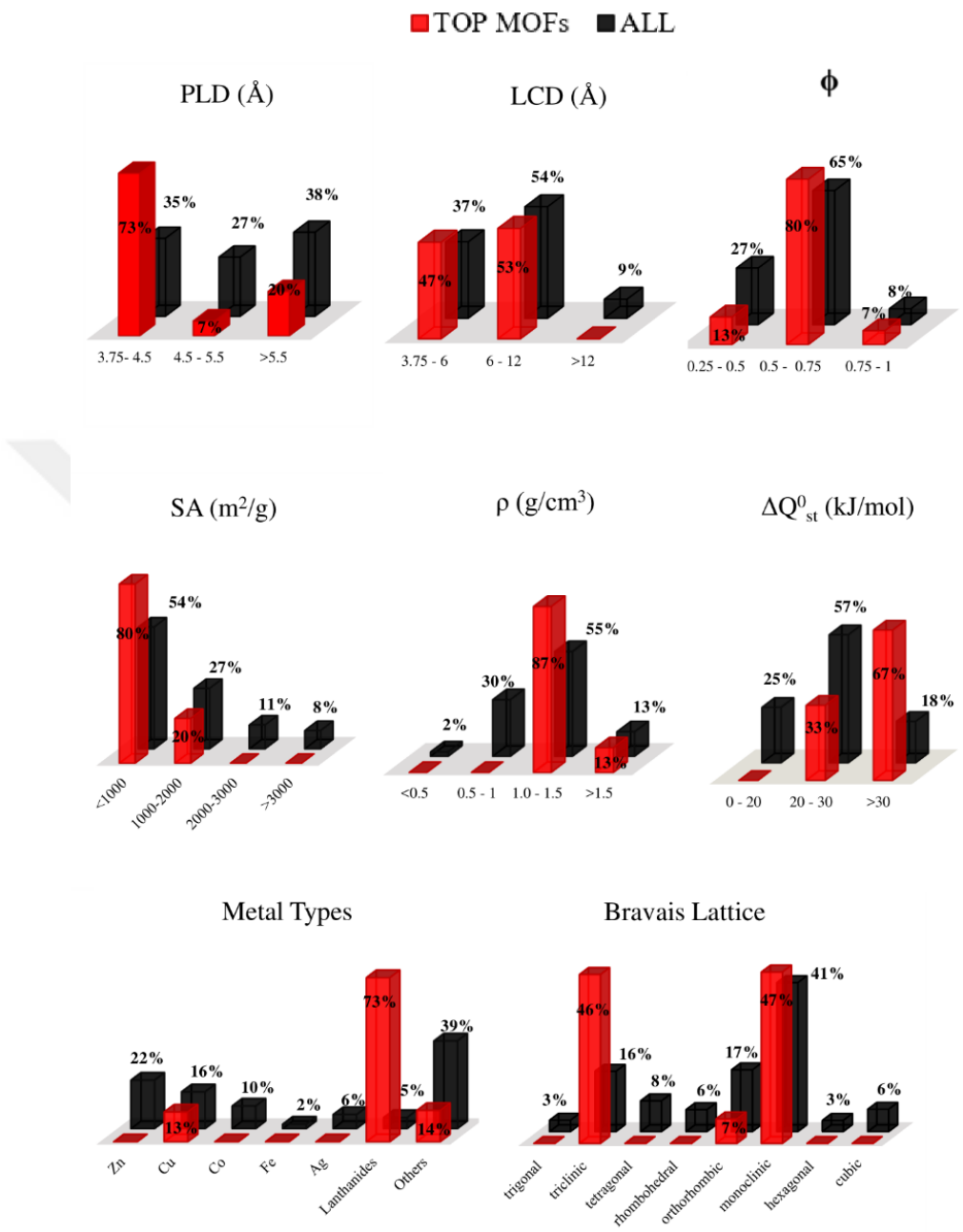

Figure 4.7. Effects of structural properties on the CO_2/N_2 separation performances of MOFs. Black columns represent all 3806 MOFs, red columns represent the top 15 MOFs that have $S^0_{mem,CO_2/N_2}$>350 and high CO_2 permeabilities, $P^0_{CO_2}$ >10^6 Barrer were chosen.

An interesting feature of Figure 4.7 is that although only a small fraction of the MOFs (190 MOFs) have lanthanides among the 3806 MOFs we considered, a significant number of the top 15 materials (11 MOFs) have lanthanides. Previous work on adsorption-based separation of CO_2/N_2 also demonstrated that MOFs with lanthanides outperform other MOFs due to the combination of high CO_2 selectivity and capacity.[40] We also examined the effect of the difference between the heat of adsorption of CO_2 and N_2 computed at infinite dilution, ΔQ^0_{st}, on the membrane performances of MOFs. In fact, ΔQ^0_{st} is not a direct structural property but it is a good representative of the affinity of the framework for adsorbate molecules. Figure 4.7 shows that although quarter of the MOF database was found to have $\Delta Q^0_{st}<20$ kJ/mol, none of these MOFs is in the top membrane list. A small portion of the MOFs, 18%, has high $\Delta Q^0_{st}>30$ kJ/mol and these MOFs become 67% of the top membranes.

This knowledge may be useful to rapidly screen MOFs after gas adsorption measurements to identify the potential membrane candidates. Overall, MOFs with $3.75<PLD<4.5$ Å, $6<LCD<12$ Å, $0.5<\phi<0.75$, $SA<1000$ m^2/g, $1.0<\rho<1.5$ g/cm^3 and the ones having lanthanides and monoclinic lattice types are the most promising MOF membranes.

Chapter 5: High-throughput Screening of MOFs as Fillers in Mixed Matrix Membranes for Flue Gas Separation[‡]

In this work, we aimed to computationally screen the recent, synthesized MOF database to evaluate the potential of all possible MOF-based MMMs for CO_2/N_2 separation. Combination of the state-of-the-art molecular simulations, grand canonical Monte Carlo (GCMC) and molecular dynamics (MD), were used to assess the single-component CO_2 and N_2 permeabilities of 7822 of MOFs and this data was then combined with the experimentally reported gas permeability data of 14 different polymers using a theoretical permeation model to predict CO_2 and N_2 permeabilities of 109508 different types of MOF/polymer MMMs. The impact of using MOF fillers on the gas separation performance of each polymer was evaluated in detail and the top 50 MOF fillers that significantly improve the CO_2/N_2 separation performances of polymers by carrying them well above the upper bound were identified. Assessing gas permeabilities of MOF-based MMMs for mixtures is important for industrial separation applications but there is very limited data on the mixture permeabilities of both MOFs and polymers. In order to unlock the flue gas separation performances of MOF-based MMMs, we computed CO_2/N_2 mixture permeabilities of the top 50 MOFs by performing molecular simulations under the same conditions with the experiments that reported mixture permeabilities of polymers. Permeabilities and selectivities of MOF/polymer MMMs for separation of binary CO_2/N_2:15/85 mixture were predicted and compared with those calculated using the single-component gas data. Finally, we investigated the impact of structural properties of MOF fillers such as porosity, pore size, accessible surface area on the CO_2/N_2 selectivity of MOF-based MMMs to provide insights into the proper selection of MOF

[‡] The results given in this chapter were published in Advanced Theory and Simulations with following reference: Daglar, H..; Keskin, S., *High-throughput Screening of MOFs as Fillers in Mixed Matrix Membranes for Flue Gas Separation.* Adv. Theory & Simul., 2019. This chapter is the reformatted version of the mentioned research paper.

fillers. These results will be useful to accelerate the design and development of new MOF-based MMMs for high-performance flue gas separation.

5.1. Validation of Predicted Results

We first compared simulated gas permeability of MOF-based MMMs with the experimental gas permeability data available in the literature. In order to be consistent with the experimental conditions, we carried out our molecular simulations under the same pressure and temperature, using the same gas composition and membrane thickness reported in the experiments. Details of these conditions are given in Table A.4 of Appendix. Figure 5.1 shows the good agreement between experimentally measured and simulated single-component CO_2 and N_2 permeabilities for 10 different MOF-based MMMs and CO_2/N_2 mixture permeabilities of 3 different MOF-based MMMs. Simulations generally underestimate the experimentally reported gas permeabilities especially as the weight percent of MOF fillers in the MMMs increases. Experimentally fabricated MMMs may have defects which may act as non-selective regions resulting in high gas permeabilities. Furthermore, the increase of the filler loading in the polymer matrix may cause agglomeration of the MOF particles in some regions of the polymer, which results in high gas permeabilities for the experimentally fabricated MOF-based MMMs.

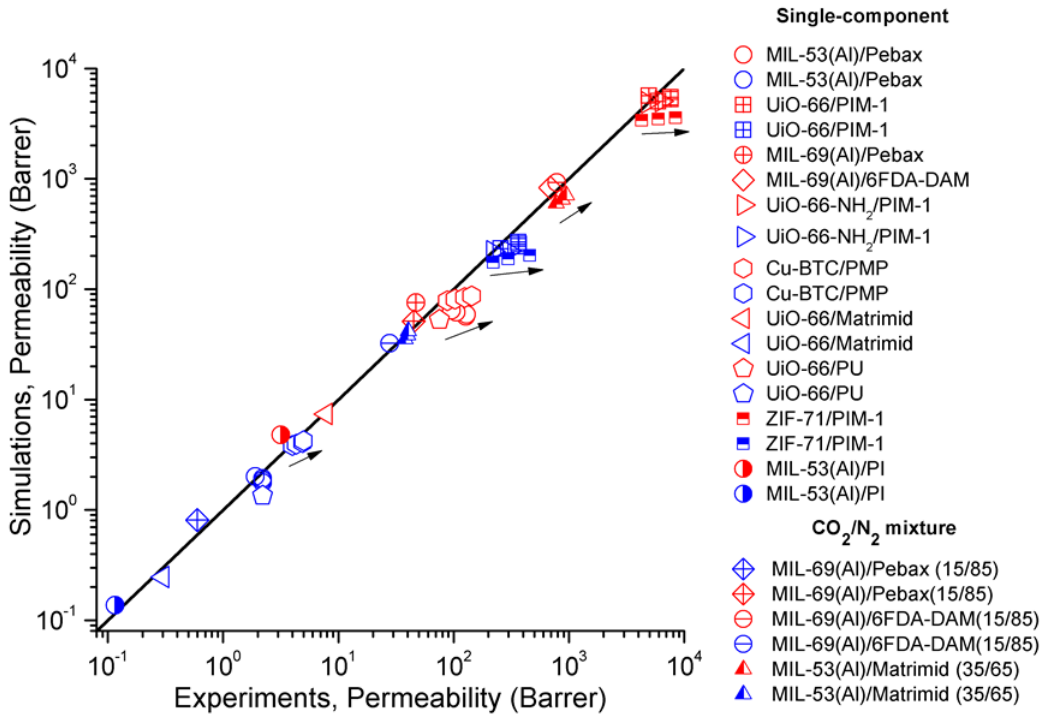

Figure 5.1. Comparison of experimental and simulated gas permeabilities of MOF-based MMMs. Red (blue) colors represent CO_2 (N_2) permeabilities of MMMs. Arrows represent increase of MOF loading in the MMM. Details of the experimental permeability measurements are given in Table A.4.

Our calculations are based on a theoretical permeation model that considers the non-ideal morphology of the MMM, however mathematical permeation models are generally limited in terms of representing the distribution and agglomeration of the filler particles in polymers especially at high filler loadings.

As shown in Figure 5.1, only a small variety of MOFs (MIL-53(Al), UiO-66, UiO-66-NH_2, Cu-BTC, ZIF-71, MIL-69(Al)) and polymers (Pebax, PIM-1, 6FDA-DAM, PMP, Matrimid, PU, PI) has been used to fabricate MOF-based MMMs to date. Therefore, we have limited data on the CO_2/N_2 separation performances of MOF-based MMMs. Considering the existence of high numbers of synthesized MOFs and polymers,

a large diversity of MMMs which may offer higher CO_2/N_2 selectivities and higher CO_2 permeabilities can exist. Motivated from the good agreement between experiments and simulations for the CO_2/N_2 separation performances of MOF-based MMMs as shown in Figure 5.1, we aimed to predict CO_2 permeabilities and CO_2/N_2 selectivities of all possible MOF/polymer MMMs for which experimental gas permeability data is not currently available. In order to predict the gas permeability of MOF-based MMMs, permeabilities of MOFs are required as described in Eq.(3.11).

5.2 Single-component Gas Screening and Selection of Top MOF Fillers

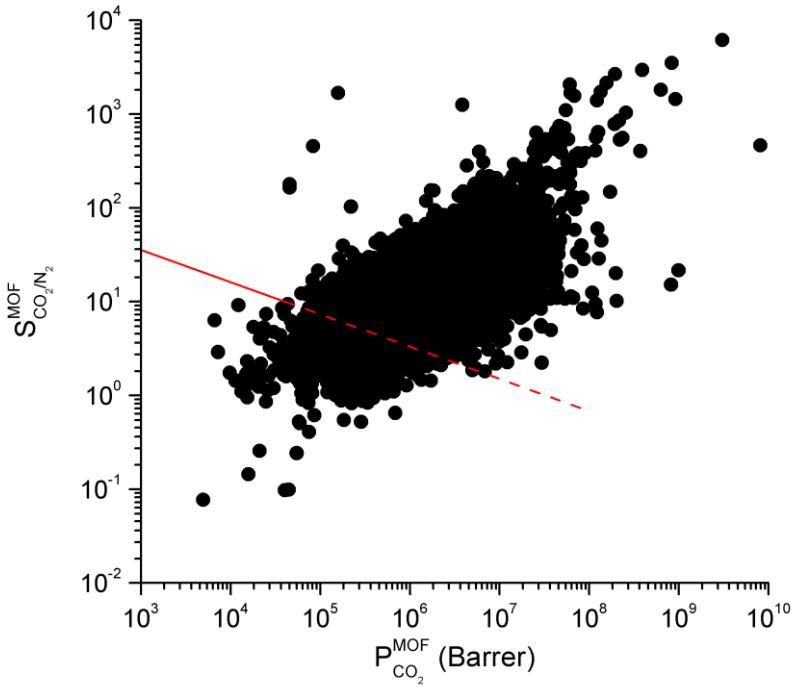

Figure 5.2. Simulated CO_2/N_2 selectivity and CO_2 permeability of MOFs computed at infinite dilution at 298 K. Red line represents the Robeson's upper bound for membrane-based CO_2/N_2 separation.

We used molecular simulations to compute CO_2 and N_2 permeabilities of 7822 MOFs at infinite dilution to save significant computation time and showed the results in Figure 5.2 together with the Robeson's upper bound. The CO_2 permeabilities of MOFs were computed to range from 4.94×10^{3} to 8.13×10^{9} Barrer whereas their CO_2/N_2 selectivities were calculated to be between 7.68×10^{-2} and 6167. The red line represents the Robeson's upper bound[8] established for the CO_2/N_2 separation performances of polymers. Experimental CO_2 permeabilities of polymers were reported to be between 5 and 7×10^{4} Barrer and CO_2/N_2 selectivities were reported to be between 8 and 220. Since MOFs generally have higher CO_2 permeabilities than the polymers, we extended the upper bound using dashed lines in Figure 5.2. These results suggest that MOFs can be promising filler particles to be used in MMM applications to enhance both the CO_2 permeabilities and CO_2/N_2 selectivities of polymers.

Using the simulation results of 7822 MOFs and experimentally reported data of 14 polymers, we predicted the CO_2 permeability and CO_2/N_2 selectivities of 109508 different MOF-based MMMs as shown in Figure 5.3. We highlight that this is the largest number of MOF-based MMMs for which synthesized, real MOFs were considered as fillers using high-throughput molecular simulations. Figure 5.3 shows that using MOFs as fillers in polymers having CO_2 permeabilities $\leq$250 Barrer, (Matrimid, Ultem, PU, Pebax, PMP, and MEEP) improves the CO_2 permeabilities of these polymers without significantly changing their CO_2/N_2 selectivities. For example, every MOF can increase the CO_2 permeability of Matrimid from 8.5 to 10.6 Barrer without changing its CO_2 selectivity. Regardless of the identity of the MOF incorporated into Matrimid, all MOF/Matrimid MMMs are located under the upper bound. In other words, none of the MOFs we examined in this work is able to carry Matrimid, Ultem, PU, Pebax, PMP above the upper bound due to the very low CO_2 permeabilities of polymers.

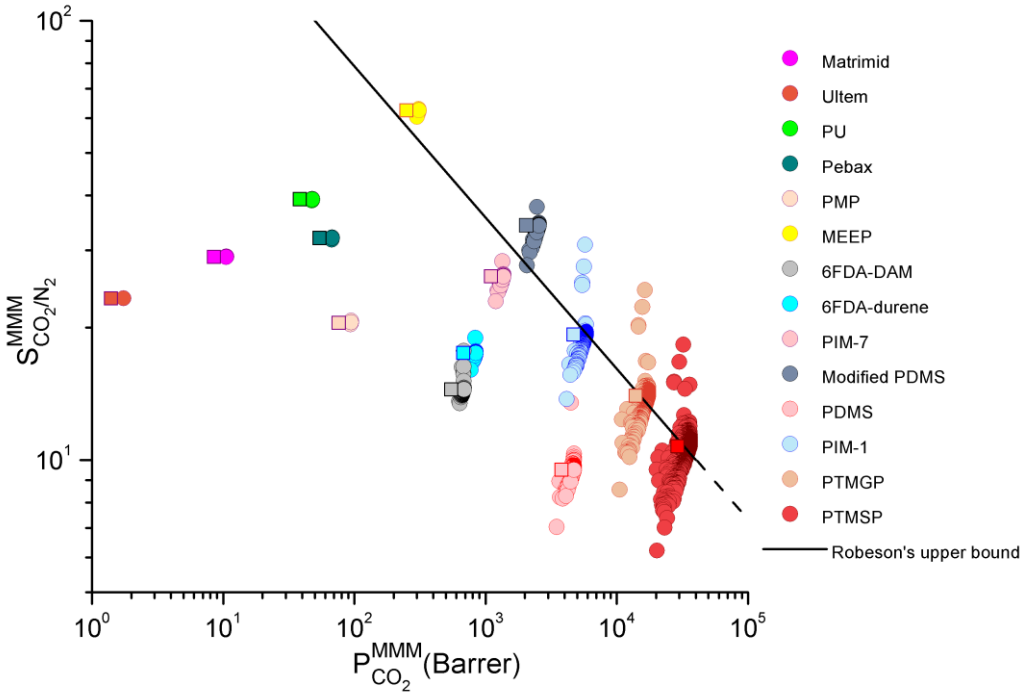

Figure 5.3. Predicted CO_2/N_2 selectivities and CO_2 permeabilities of 109508 MOF-based MMMs. The squares (circles) represent pure polymers (MOF-based MMMs).

6FDA-DAM, 6FDA-durene, PIM-7, and modified PDMS represent the polymers having CO_2 permeabilities between 550 and 2050 Barrers. The CO_2 permeabilities of these polymers increase upon the incorporation of MOF fillers while CO_2/N_2 selectivities of MOF-based MMMs become either higher or lower than those of pristine polymers. For instance, the CO_2 permeability of PIM-7 is 1100 Barrer while the CO_2 permeabilities of MOF/PIM-7 MMMs range from 1200 to 1369 Barrer, showing the permeability improvement upon the incorporation of MOF fillers into the polymer. The CO_2/N_2 selectivity of PIM-7 membrane is 26.2 whereas selectivities of MOF/PIM-7 MMMs were computed to be in the range of 23-32.5, indicating that some MOF fillers enhance the selectivity of PIM-7 whereas some other MOFs may decrease it. Finally, we examined the effect of using MOF fillers in the polymers having already high CO_2 permeabilities,

>3000 Barrer, such as PDMS, PTMSP, PIM-1, and PTMGP. Figure 5.3 shows that the identity of the MOF is very important for these polymers because MOFs can increase or decrease both CO_2 permeabilities and CO_2/N_2 selectivities. For example, PTMSP has the highest CO_2 permeability, 29000 Barrer, among the 14 polymers we studied. The CO_2 permeabilities of MOF/PTMSP MMMs were computed to be 20294-36102 Barrers, showing that some MOF fillers improve the CO_2 permeability whereas some others decrease it. The CO_2/N_2 selectivity of MOF/PTMSP MMMs was calculated to be between 6.2 and 18.3 whereas selectivity of the pure polymer was 10.7. This example shows the importance of the appropriate selection of MOF for the polymers offering high permeability but suffering from low selectivity.

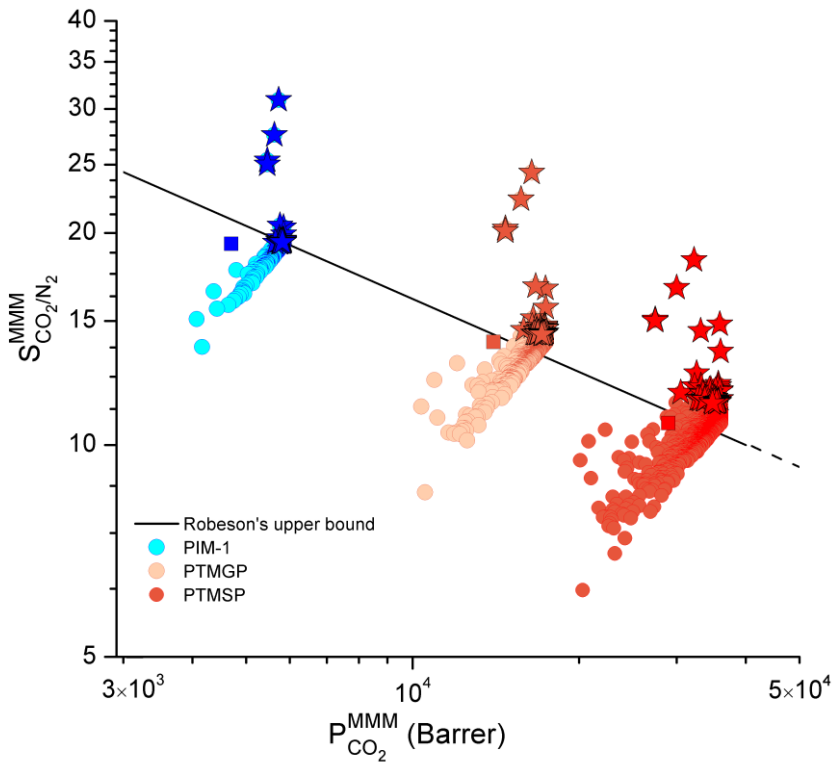

Figure 5.4. Predicted CO_2/N_2 selectivities and CO_2 permeabilities of MOF-based MMMs composed of PIM-1, PTMGP, and PTMSP. The stars represent the top 50 MOF fillers providing the highest CO_2/N_2 selectivity for MMMs.

The most important feature of Figure 5.3 is that PIM-1, PTMSP, and PTMGP are the polymers that are close to the upper bound and with the addition of some MOF fillers, MMMs of these polymers can exceed the upper bound. Therefore, we specifically focused on these three polymers in Figure 5.4 and identified the top 50 common MOF fillers that lead to MMMs having the highest CO_2/N_2 selectivities. Stars in Figure 5.4 show the top 50 MOF fillers that significantly enhance the CO_2/N_2 separation performances of PIM-1, PTMGP and PTMSP in MMM applications and the refcodes of the top 50 MOF fillers are given in Table A.5. For example, CO_2 permeability and CO_2/N_2 selectivity of PIM-1 are 4700 Barrer and 19.3, respectively, locating this polymer under the upper bound. We predicted the CO_2 permeabilities and CO_2/N_2 selectivities of MOF/PIM-1 MMMs composed of the best 50 MOF fillers in the range of 5462-5848 Barrers and 19.4-31, respectively. Due to the enhanced CO_2 permeabilities and selectivities, MOF/PIM-1 MMMs exceed the upper bound. Similarly, the same 50 MOF fillers enhanced the CO_2 permeability of PTMGP from 14000 Barrer to 14711-17402 Barrers. Except 2 MOFs, the CO_2 permeability of PTMSP also increased from 29000 Barrer to a range of 30010-35986 Barrers. The CO_2/N_2 selectivity of PTMGP (PTMSP) also increased from 14 (10.7) to 14.3-24.4 (11.5-18.3) with the addition of the top MOF fillers. We note that MMMs composed of PTMGP and PTMSP and the top 50 MOFs all exceed the upper. It is also important to note that achievable gas permeability of a MOF-based MMM that we predicted is actually limited by the theoretical permeation model. If the gas permeability of the MOF is significantly higher than that of the polymer, $P^{MOF} >> P^{P}$, then the modified Felske model given in Eq.(3.11) reduces to $P^{MMM} = P^{P} \times 1.24$ at a filler volume fraction of 0.3. That means the maximum achievable gas permeability of a MOF-based MMM is 1.24 times higher than that of the polymer.

5.3. Binary Mixture Simulations

We so far predicted CO_2/N_2 separation performances of MOF-based MMMs using the single-component gas simulation data of MOFs performed at infinite dilution and using the experimentally reported single-component gas permeability data of polymers.

This approach was used because (a) pure gas permeabilities of polymers are commonly measured and reported in the literature due to the complexity of multi-component mixture permeability measurements, (b) performing mixture simulations for thousands of MOF fillers at a pre-defined pressure is computationally much more expensive compared to performing single-component gas simulations at infinite dilution where the adsorbate-adsorbate interactions are neglected. It would be very useful to assess the CO_2/N_2 mixture separation performances of MOF-based MMMs under practical operation conditions to unlock their real potentials for industrial applications. With this motivation, we performed molecular simulations of adsorption and diffusion of CO_2/N_2:15/85 mixtures at 1 bar, 298 K for the top 50 MOF fillers.

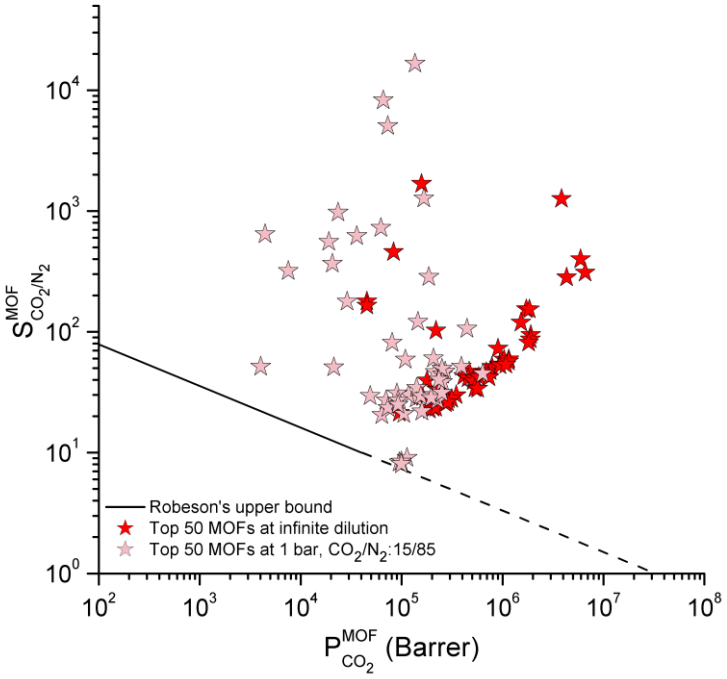

Figure 5.5. Predicted CO_2/N_2 selectivities and CO_2 permeabilities of the top 50 MOFs using single-component gas simulations performed at infinite dilution and using binary CO_2/N_2 mixture simulations performed at 1 bar, 298 K.

Figure 5.5 compares the CO_2/N_2 selectivities and CO_2 permeabilities of the top 50 MOFs computed at mixture conditions with those calculated at infinite dilution. MOFs generally have lower CO_2 permeabilities (4.03×10^3-6.34×10^5 Barrer) and lower N_2 permeabilities (6.9-1.41×10^4) at the binary mixture conditions compared to CO_2 permeabilities (4.54×10^4-6.6×10^6 Barrer) and N_2 permeabilities (9.4×10^1-2.23×10^4) computed at infinite dilution. Since the decrease in N_2 permeabilities is more pronounced than the decrease in CO_2 permeabilities, higher CO_2/N_2 selectivities (8-16628) were generally observed at binary mixture conditions compared to the ones computed at infinite dilution (21-1679). The decrease in the gas permeabilities can be explained by the decreases in the adsorption amounts and self-diffusivities of the gas components due

to the competition between CO_2 and N_2 molecules.[109] An important result of Figure 5.5 is that the best 50 MOFs were still above the upper bound when their permeabilities were computed using the mixture simulations. This indicates that screening the MOFs at infinite dilution condition using the single-component gas simulations is an efficient strategy to quickly identify the best MOFs for the separation of binary CO_2/N_2 mixture.

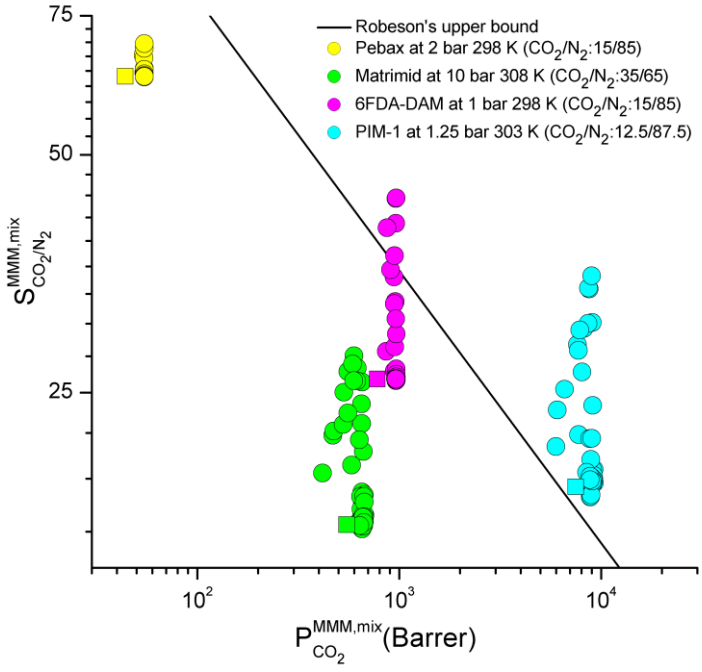

Figure 5.6. Predicted CO_2/N_2 selectivities and CO_2 permeabilities of MOF-based MMMs for mixture separation. The squares (circles) represent gas permeability and selectivity of polymers (MOF-based MMMs).

In order to estimate the CO_2/N_2 mixture separation performances of MOF/polymer MMMs, we collected available mixture permeability data of polymers from the literature. Gas permeabilities of Matrimid, Pebax, 6FDA-DAM and PIM-1 were experimentally reported at different pressures for different gas compositions. We performed GCMC and

MD simulations of MOFs under the same conditions with these experiments. Figure 5.6 shows the CO_2 permeabilities and CO_2/N_2 selectivities of 200 MOF-based MMMs composed of the top 50 MOF fillers and 4 polymers, Pebax, 6FDA-DAM, Matrimid, and PIM-1. This is the largest number of MOF-based MMMs for which CO_2/N_2 mixture separation performances were predicted. Results shown in Figure 5.6 indicate that MOF/polymer MMMs are promising for the separation of binary CO_2/N_2 mixtures with various compositions. For example, the CO_2 permeability and CO_2/N_2 selectivity of Pebax were reported as 44 Barrer and 63, respectively, at 2 bar, 298 K for CO_2/N_2:15/85 mixture.[73] The CO_2 permeabilities and CO_2/N_2 selectivities of MOF/Pebax MMMs were predicted as ~54 Barrer and 63-67, respectively, showing both the permeability and selectivity improvement upon the incorporation of MOF fillers. However, these improvements were not enough to carry the Pebax above the upper bound. The CO_2 permeability and CO_2/N_2 selectivity of Matrimid were measured as 550.3 Barrer and 17, respectively, at 10 bar, 308 K for the separation of CO_2/N_2:35/65 mixture.[110] Predicted CO_2 permeabilities and CO_2/N_2 selectivities of MOF/Matrimid MMMs were in the range of 418-676 Barrers and 16.8-27.9, respectively, but these improvements were not enough to locate the Matrimid-based MMMs above the upper bound. The CO_2 permeability and CO_2/N_2 selectivity of 6FDA-DAM were reported as 780 Barrer and 26, respectively, at 1 bar, 298 K for separation of CO_2/N_2:15/85 mixture.[111] We predicted CO_2 permeabilities of MOF/6FDA-DAM MMMs in the range of 863-970 Barrer and CO_2/N_2 selectivities as 26-44 under the same operating conditions. These results showed the positive effect of using MOF fillers on the CO_2/N_2 mixture separation performance of 6FDA-DAM. Figure 5.6 also shows that 4 MOFs could carry 6FDA-DAM membrane above the Robeson's upper bound. The CO_2 permeability and CO_2/N_2 selectivity of PIM-1 were reported as 7500 Barrer and 19, respectively, at 1.25 bar 303 K for the separation of CO_2/N_2:12.5/87.5 mixture.[112] We predicted CO_2 permeabilities and CO_2/N_2 selectivities of MOF/PIM-1 MMMs as 5976-9256 Barrer and 18.4-35.2, respectively. Some MOFs were found to increase the CO_2 permeability of PIM-1 at the expense of a

slight decrease in its selectivity and all MOF/PIM-1 membranes are located above the upper bound.

For the 4 polymers that we studied in Figure 5.6, single-component gas permeability data also exist in the literature and we compared the predicted gas permeabilities of MOF-based MMMs composed of these polymers at single-component and mixture cases. Although operating pressure, temperature and composition of the gas mixtures are different for the polymeric membranes, Table 5.1 shows that CO_2 permeabilities and CO_2/N_2 selectivities of MOF-based MMMs that we computed at mixture conditions are generally higher than the ones computed at single-component gas condition. For example, for MOF/6FDA-DAM MMMs, the maximum CO_2 permeability and CO_2/N_2 selectivity was predicted as 684.7 Barrer and 17.7 at single-component gas conditions at 1 bar, 298 K. The maximum value of CO_2 permeability and selectivity of MOF/6FDA-DAM MMMs were calculated as 970.2 Barrer and 44.1, respectively for the separation of CO_2/N_2:15/85 mixture under the same pressure and temperature. The higher CO_2 permeability and selectivity of MMMs at mixture condition compared to the single-component gas condition can be explained by the higher CO_2 permeability and selectivity of pristine polymer. For example, Jorge and coworkers[111] reported both the single-component and mixture permeabilities of 6FDA-DAM and showed that CO_2 permeability increased from 550 to 780 Barrer when CO_2/N_2 mixture was considered whereas N_2 permeability decreased from 38 to 30 Barrer because of the higher solubility of CO_2 in glassy polymers, resulting in higher mixture selectivity than the ideal selectivity. Similar discussion is valid for PIM-1. Single-component CO_2 and N_2 permeabilities of PIM-1 were measured as 4700 and 243 Barrers, respectively.[113] We predicted single-component CO_2 and N_2 permeabilities of MOF/PIM-1 MMMs as 5462-5849 Barrers and 185-301 Barrers, respectively with ideal CO_2/N_2 selectivities of 19.4-30.9 as shown in Figure 5.3. For CO_2/N_2:12.5/87.5 mixture, CO_2 and N_2 permeability of PIM-1 were measured as 7500 and 395 Barrer, respectively.[112] Mixture CO_2 and N_2 permeabilities of MOF/PIM-1 MMMs were predicted as 5976-9256 and 255-482 Barrers, respectively. Mixture selectivity of MOF/PIM-1 MMMs was calculated to vary between 18.4-35.2

whereas that of PIM-1 was 19. These results show that the maximum achievable CO_2 permeability and CO_2/N_2 selectivity of MOF/PIM-1 MMMs for separation of CO_2/N_2 mixture are higher than those computed for single-component gas separation.

Table 5.1. Comparison of separation performances of 4 polymers that have both single-component and mixture permeability measurements.

Polymer	Condition	$P^P_{CO_2}$ (Barrer)	$P^P_{N_2}$ (Barrer)	$S^P_{CO_2/N_2}$	$P^{MMM}_{CO_2}$ (Barrer)		$P^{MMM}_{N_2}$ (Barrer)		$S^{MMM}_{CO_2/N_2}$	
					Max.	Min.	Max.	Min.	Max.	Min.
Pebax	SG 10 bar, 308 K	54.4	1.7	32.0	67.7	67.7	2.1	2.1	32.4	32.0
Pebax	GM (15/85) 2 bar, 298 K	44.0	0.7	62.9	54.8	54.4	0.9	0.8	66.8	62.8
Matrimid	SG Isochoric, 295 K	8.5	0.2	29.0	10.6	10.6	0.3	0.3	29.0	29.1
Matrimid	GM (35/65) 10 bar, 308 K	550.3	32.4	17.0	676.1	417.5	39.4	30.0	27.9	16.8
6FDA-DAM	SG 1 bar, 298 K	550	38	14.5	684.7	678.6	47.3	38.5	17.7	14.5
6FDA-DAM	GM (15/85) 1 bar, 298 K	780.0	30.0	26.0	970.2	863.2	37.3	21.5	44.1	25.9
PIM-1	SG Isochoric, 313 K	4700.0	243.0	19.3	5849.4	5462.1	300.7	185.4	30.9	19.4
PIM-1	GM (12.5/87.5) 1.25 bar, 303 K	7500.0	395.0	19.0	9256.4	5975.7	481.9	255.1	35.2	18.4

* SG: Single-component gas, GM: Gas mixture.

5.4 Structure-Performance Relationships of MOF-based MMMs

We finally aimed to reveal the relations between the structural properties of MOF fillers and overall gas separation performance of MOF-based MMMs. Since MOF-based MMMs composed of PIM-1 have the widest range of CO_2/N_2 selectivities, we specifically focused on this polymer to investigate the effect of structural properties of MOFs on the selectivity of MOF/PIM-1 MMMs. Figure 5.7 shows the porosity of MOFs as a function of their pore sizes and accessible surface areas and we color-coded 7822 MOFs based on CO_2/N_2 selectivities of MOF/PIM-1 MMMs computed at infinite dilution. In each figure, red symbols show MOF/PIM-1 MMMs having CO_2/N_2

selectivities (13.8-19.3) lower than the selectivity of PIM-1 (19.3). The MOFs used as fillers in these MMMs have a very wide range of LCDs (4.09-71.64 Å), PLDs (3.75-71.50 Å), porosities (0.32-0.94) and surface areas (41.84-22299 m^2/g). Green symbols show MOF/PIM-1 MMMs having almost similar CO_2/N_2 selectivity (19.3-19.5) with that of PIM-1. These MOFs have relatively narrower LCD (PLD) ranges between 3.92-26.78 Å (3.75-25.49 Å), narrower porosities (0.28-0.86) and lower accessible surface areas (13.44-10239) than the MOFs shown with red color. Blue symbols represent MOF/PIM-1 MMMs having significantly higher CO_2/N_2 selectivities (19.5-30.9) than the selectivity of pristine PIM-1. These MOFs have a narrow range of LCDs (4.62-7.48 Å), PLDs (3.75-5.12 Å), porosities (0.41-0.55) and surface areas (81.38-784.54 m^2/g). Figure 5.7(a) shows that as the porosity and LCD of MOFs decrease, the CO_2/N_2 selectivities of MOF/PIM-1 MMMs increase. The MMMs composed of the top 50 MOF fillers are shown with stars. The top 50 MOF fillers that offer the highest CO_2/N_2 selectivities possess porosities between 0.41 and 0.58 and LCDs between 4.2-7.5 Å. Similarly, Figure 5.7(b) shows that MOFs having narrow PLDs, 3.75-5.12 Å, with low porosities also result in highly selective MMMs. None of the MOFs having large pore sizes (LCD>12 Å, PLD>6 Å) leads to highly selective MMMs. Finally, Figure 5.7(c) shows that MOFs having accessible surface areas of 81.4-934 m^2/g are the best fillers for highly selective MMMs.

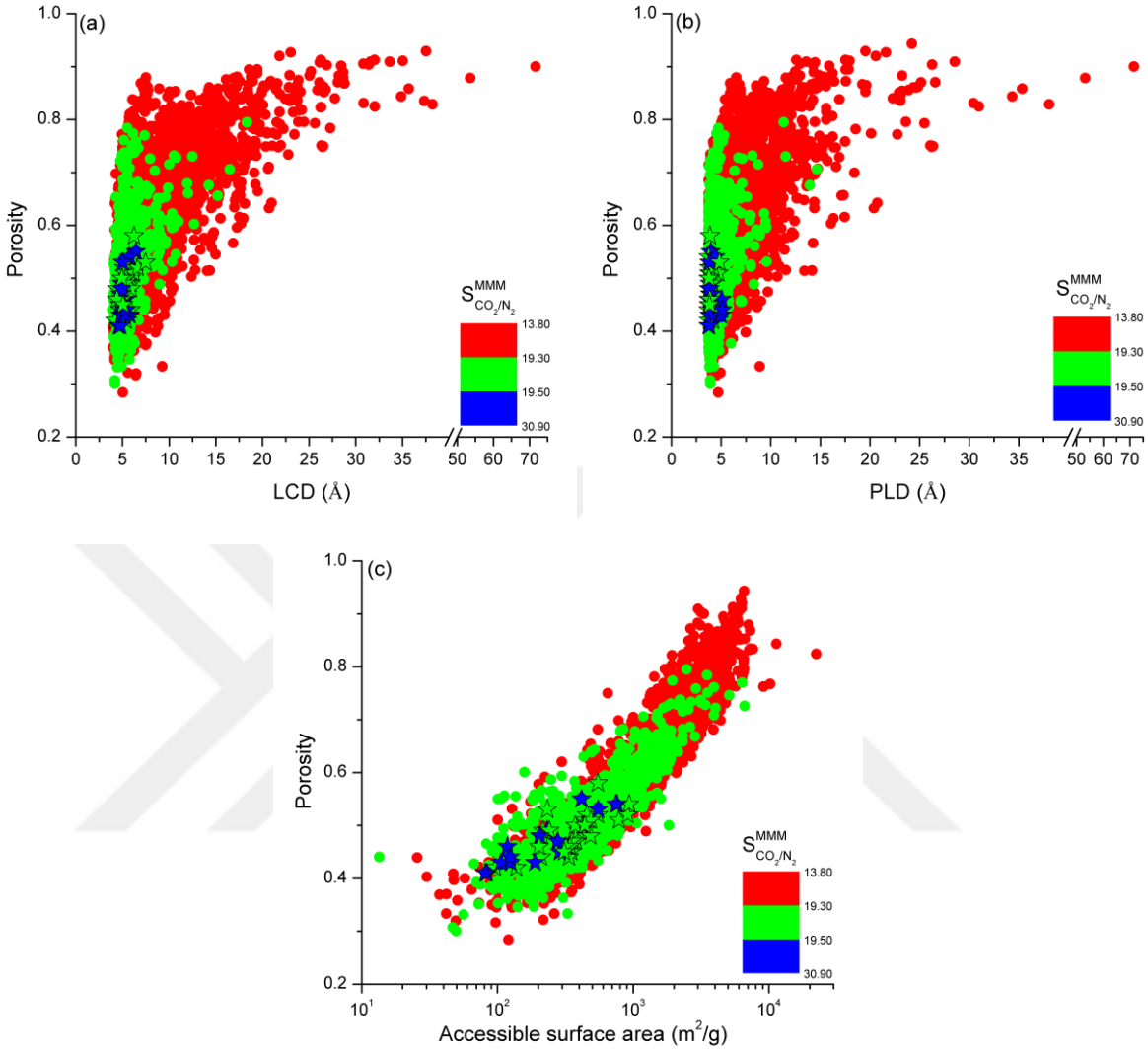

Figure 5.7. Porosity as a function of (a) LCD, (b) PLD (c) accessible surface area of 7822 MOFs. The color scaling represents the CO_2/N_2 selectivity of MOF/PIM-1 MMMs and stars represent the MMMs composed of the top 50 MOF fillers.

At that point we would like to note that gas separation performance of MMMs depends on several factors other than the structural properties of MOF fillers that we examined in Figure 5.7. For example, all our calculations predicting the gas separation

performances of MOF/polymer MMMs simply assume that there is no specific compatibility problem between the MOF and the polymer such as no-adhesion between the polymer and MOF phases. In fact, the MOF/polymer interface dictates the feasibility and stability of the MMMs, therefore fundamental understanding of this interface is critical. Several excellent studies described the computational methods combining the density functional theory (DFT) calculations and MD simulations to model MOF/polymer interfaces,[114-116] which can be used to examine the potential affinity between different MOF surfaces and polymers once the appropriate force field representing the correct description of the MMM is defined. It is also important to note that all our results are for single-component and binary mixture permeabilities of MOF-based MMMs and we neglected the presence of H_2O in the flue gas stream. In Chapter 4, we showed the presence of humidity can reduce both the CO_2 and N_2 permeabilities of pure MOF membranes. In an experimental study,[112] the decrease in CO_2 and N_2 permeabilities was observed in the presence of water. Based on these studies, one can expect lower CO_2 and N_2 permeabilities for the MOF-based MMMs in the presence of humidity. We believe that after the best MOF candidates are computationally identified for MMM applications, it is more likely to investigate the compatibility, stability and reusability issues of membranes using experimental manners.

Chapter 6: Conclusions and Outlook

As a result of human activity, CO_2 emission has become a big problem to solve by researchers. Especially, flue gas which is an exhaust gas in the industry has been considered as one of the biggest reasons of CO_2 emission. For the last two-decade, MOFs have been accepted as remarkable materials for CO_2 separation process because of the variety of pore sizes and the presence of very large number of structures. The large number of MOFs has directed researchers to computational screening in order to save time, resource and energy. In this thesis, computational screening methods, mainly molecular simulations have been used to investigate the gas separation performances of MOFs and MOF-based MMMs.

In the first part, we used high-throughput molecular simulations to screen the most recent MOF database for membrane-based CO_2/N_2 separations. Single-component gas adsorption and diffusion calculations performed at infinite dilution were used to assess CO_2 permeabilities and CO_2/N_2 selectivities of MOF membranes. Adsorption and diffusion of binary CO_2/N_2 mixtures in MOFs were then computed for the top MOFs identified from the first level of screening under post-combustion CO_2 separation conditions. Top 15 MOF membranes were found to exhibit CO_2 selectivities of 15-820 and CO_2 permeabilities of 3.57×10^3-1.95×10^6 Barrers for the separation of CO_2/N_2:15/85 mixture at 1 bar and 298 K. High membrane selectivities of MOFs were attributed to the strong adsorption affinity towards CO_2 which dominated diffusion selectivity towards N_2. We finally examined ternary $CO_2/N_2/H_2O$ mixtures to better assess separation performances of the selected top membranes. Results showed that selectivities and permeabilities calculated from the ternary mixture simulation are generally lower than the values computed using binary mixture simulations, indicating that humidity can negatively affect the performances of MOF membranes. Structure-performance analysis demonstrated that pure MOF membranes with narrow pores (3.75<PLD<4.5 Å), low

surface areas (<1000 m^2/g), monoclinic and lanthanides-containing structures are the best candidates for CO_2/N_2 membrane-based gas separation.

In the second part, CO_2/N_2 separation performances of a very large number (109508) of MOF-based MMMs composed of 7822 different types of MOFs and 14 different polymers were predicted by using high-throughput molecular simulations. Among the MOF-based MMMs that we examined, the maximum CO_2/N_2 selectivity was computed as 64.3 and the highest CO_2 permeability was estimated as 36103 Barrers. It has been recently discussed that CO_2/N_2 selectivity greater than 50 and CO_2 permeability over 100 Barrer are required for an economic operation of CO_2 capture from flue gas.[117] There are several MOF-based MMMs which were predicted to have CO_2/N_2 selectivities and CO_2 permeabilities well beyond these desired values, highlighting the great potential of using MOFs as fillers in polymer membranes. Many MOFs can improve both the selectivity and permeability of 6FDA-DAM, 6FDA-durene, PIM-7, PDMS, modified PDMS, PIM-1, PTMGP, PTMSP. Since highly permeable PIM-1, PTMGP and PTMSP are very close to the upper bound, using MOFs as fillers in these polymers results in exceeding the Robeson's upper bound. We also examined binary CO_2/N_2 mixture separation performances of MOF-based MMMs and showed that MOFs have a great potential to improve the mixture selectivity of 6FDA-DAM from 26 to 44.1 and PIM-1 from 19 to 35.2. We finally showed that selecting MOF fillers with narrow pore sizes and low porosities lead to MMMs exhibiting high CO_2/N_2 selectivities.

In this thesis, some assumptions were used throughout computational screening. Firstly, rigid MOF assumption was used in all molecular simulations. This assumption saves tremendous computational time and it is necessary for large-scale screening studies which consider thousands of MOF structures. On the other hand, the rigid framework assumption may overpredict the diffusion selectivity towards small gas molecule (CO_2) by underestimating diffusion of large gas molecule (N_2). Erucar and Keskin[118] previously presented that MOF flexibility has an insignificant effect on the selectivity and permeability of MOF structures having large pores whereas it affected permeability

without varying selectivity for materials having narrow pores. In this thesis, we specifically considered MOFs having pore openings greater than the kinetic diameters of the adsorbates (CO_2 and N_2), hence it can be expected that MOF flexibility has a negligible effect on the results of this thesis. Another point is that Qeq method was used to assign partial charges to MOFs since this approximate was readily implemented within RASPA. The good agreement between experiments and our molecular simulations for CO_2 and N_2 permeabilities of several MOF membranes indicated that Qeq method can accurately estimate properties of MOF membranes and MOF-based MMMs, respectively. Furthermore, it was recently showed that adsorption selectivities do not significantly change depending on the method by comparing the results of GCMC simulations using Qeq and density-derived electrostatic and chemical charge method (DDEC).[119]

In addition to these assumptions, all our calculations predicting the gas separation performances of MOF/polymer MMMs simply assume that there is no specific compatibility problem between the MOF and the polymer such as no-adhesion between the polymer and MOF phases. In fact, the MOF/polymer interface dictates the feasibility and stability of the MMMs, therefore fundamental understanding of this interface is critical. Several excellent studies described the computational methods combining the density functional theory (DFT) calculations and MD simulations to model MOF/polymer interfaces,[114-116] which can be used to examine the potential affinity between different MOF surfaces and polymers once the appropriate force field representing the correct description of the MMM is defined. It is also important to note that all results given in Chapter 5 were for single-component and binary mixture permeabilities of MOF-based MMMs and we neglected the presence of H_2O in the flue gas stream. In Chapter 4, the results of ternary $CO_2/N_2/H_2O$ mixture simulation showed the presence of humidity can reduce both the CO_2 and N_2 permeabilities of pure MOF membranes. In an experimental study,[112] the decrease in CO_2 and N_2 permeabilities was observed in the presence of water. Based on these studies, one can expect lower CO_2 and N_2 permeabilities for the MOF-based MMMs in the presence of humidity.

As a conclusion, MOFs are considered as promising both as pure membranes and as fillers for MMMs in gas separation applications. It is important to note that research area in the way of identifying the top MOFs is growing fast and the gas separation performance data of MOFs has been widened. Thus, it is possible to identify the best MOF membrane or MOF/polymer MMMs which can outstandingly perform as an energy efficient material for flue gas separation. In order to estimate promising MOF membrane and MOF/polymer MMM membranes for gas adsorption and separation applications with higher accuracy, there are many directions that can be considered as the future work:

Fully atomistic modelling approach of MMMs where the MOF and polymer are simulated together is important subject for future studies since they provide deep exploration of the interfacial interactions between MOF filler and polymer matrix in computational studies. In addition to this, fully atomistic simulations are better in representing the real conditions in which a polymer may easily pack with a flexible MOF designed as fillers compared to rigid MOF simulations. These simulations can also be performed for sorption, diffusion and permeation of gas molecules in MMMs separately by the way of modelling not only MOF filler but also polymer matrix. To the best our knowledge, there is a very limited number of studies on fully atomistic simulations because of their computational cost and complexity. Jiang et al.[120] performed fully atomistic simulations for H_2/CO_2 separation in MMM composed of ZIF-7 and polybenzimidazole (PBI) for the first time. They used a complex force field considering flexibility to describe ZIF-7 atoms. Their simulated permeabilities of CO_2 and H_2 were relatively different from experimental results because of the difficulties in representing all interfacial interactions between MOF and polymer. To deeply understand interfacial interactions between MOF and polymer, Maurin et al.[121] focused on the microscopic model of ZIF-8/PIM-1 MMM using a hybrid computational methodology integrating quantum and force field simulations. They used DFT optimization for MOF surface and 21 MD equilibration steps for polymer surface. Then, after combining of optimized MOF and equilibrated polymer, they also repeated 21 MD steps for equilibration of ZIF-8/PIM-1 MMM. Because of the complexity of performed simulations, their results are valuable

for the literature. It is not straightforward to apply fully atomistic modelling approach for high throughput screening of thousands of MOF/polymer MMMs because of the computational cost. Instead of this, fully atomistic modelling approach can be applied to a small number of MMMs which are selected as promising material from initial computational screening approach.

Experimental testing of pure MOF membranes and MOF-based MMMs is another important issue because the majority of computational studies about MOF membranes assume the ideal and nondefective crystal structures. Sholl et al.[122] reviewed that MOFs have generally two different types of defects which are point defects associated with metallic or organic parts of MOF and extended defects associated with imperfections in the structure. These defects that are not considered in computational studies may cause to stability and feasibility problems. In addition to this, computational studies generally assume that used MOF materials are fully activated meaning that the structures are exactly solvent-free. However, in fabricating process, removal of solvent molecules could not be completed. In summary, the results of computational studies offer promising MOF/polymer combinations that can form the best MMMs, but it may not be possible to combine them in practice because of their different chemical and mechanical stabilities. In future studies, these issues can be investigated to assess the full potential of the best MOF membrane and MOF/polymer MMMs.

REFERENCES

[1] Tollefson, J., World's Carbon Emissions. *Nature News,* **2017**, 551(7680), 283.

[2] Granite, E.J. and T. O'Brien, Review of novel methods for carbon dioxide separation from flue and fuel gases. *Fuel Process. Technol.,* **2005**, 86(14-15), 1423-1434.

[3] Brunetti, A., et al., Membrane technologies for CO2 separation. *J. Membrane Sci.,* **2010**, 359(1), 115-125.

[4] Kim, S. and Y.M. Lee, High performance polymer membranes for CO2 separation. *Curr. Org. Chem. Eng.,* **2013**, 2(2), 238-244.

[5] Dai, Z., L. Ansaloni, and L. Deng, Recent advances in multi-layer composite polymeric membranes for CO2 separation: A review. *Green Energy & Environment,* **2016**, 1(2), 102-128.

[6] Ahmad, J., et al., Recent Advances in Poly (Amide-B-Ethylene) Based Membranes for Carbon Dioxide (CO2) Capture: A Review. *Polym-Plast. Technol.,* **2019**, 58(4), 366-383.

[7] Feng, S., et al., Effect of poly(ethylene glycol) molecular weight on CO2/N2 separation performance of poly(amide-12-b-ethylene oxide)/poly(ethylene glycol) blend membranes. *J. Energy Chem,* **2019**, 28, 39-45.

[8] Robeson, L.M., The upper bound revisited. *J. Membrane Sci.,* **2008**, 320(1-2), 390-400.

[9] Long, J.R. and O.M. Yaghi, The Pervasive Chemistry of Metal-Organic Frameworks. *Chem. Soc. Rev.,* **2009**, 38(5), 1213-1214.

[10] Furukawa, H., et al., The Chemistry and Applications Of Metal-Organic Frameworks. *Science,* **2013**, 341(6149), 974-+.

[11] Bon, V., I. Senkovska, and S. Kaskel, *Nanoporous Materials for Gas Storage*. 2019: Springer. 137-172.

[12] Yu, J., et al., CO_2 capture and separations using MOFs: computational and experimental studies. *Chem. Rev.,* **2017**, 117(14), 9674-9754.

[13] Ding, M., et al., Carbon capture and conversion using metal–organic frameworks and MOF-based materials. *Chem. Soc. Rev.,* **2019**.

[14] Qiu, S.L., M. Xue, and G.S. Zhu, Metal-Organic Framework Membranes: From Synthesis to Separation Application. *Chem. Soc. Rev.* , **2014**, 43(16), 6116-6140.

[15] Groom, C.R., et al., The Cambridge structural database. *Acta. Cryst. B: Struc. Sci.,* **2016**, 72(2), 171-179.

[16] Ben-Mansour, R., et al., Carbon capture by physical adsorption: materials, experimental investigations and numerical modeling and simulations–a review. *Appl. Energy,* **2016**, 161, 225-255.

[17] Galizia, M., et al., 50th anniversary perspective: Polymers and mixed matrix membranes for gas and vapor separation: A review and prospective opportunities. *Macromolecules,* **2017**, 50(20), 7809-7843.

[18] Lin, R., et al., Metal organic framework based mixed matrix membranes: an overview on filler/polymer interfaces. *J. Mater. Chem. A,* **2018**, 6(2), 293-312.

[19] Rezakazemi, M., et al., State-of-the-art membrane based CO_2 separation using mixed matrix membranes (MMMs): an overview on current status and future directions. *Prog. Polym. Sci.*, **2014**, 39(5), 817-861.
[20] Zornoza, B., et al., Metal organic framework based mixed matrix membranes: An increasingly important field of research with a large application potential. *Microporous Mesoporous Mater.*, **2013**, 166, 67-78.
[21] Seoane, B., et al., Metal–organic framework based mixed matrix membranes: a solution for highly efficient CO2 capture? *Chem. Soc. Rev.*, **2015**, 44(8), 2421-2454.
[22] Jiang, J.W., R. Babarao, and Z.Q. Hu, Molecular Simulations for Energy, Environmental and Pharmaceutical Applications of Nanoporous Materials: From Zeolites, Metal-Organic Frameworks to Protein Crystals. *Chem. Soc. Rev.*, **2011**, 40(7), 3599-3612.
[23] Adatoz, E., A.K. Avci, and S. Keskin, Opportunities and challenges of MOF-based membranes in gas separations. *Sep. Purif. Technol.* , **2015**, 152, 207-237.
[24] Phan, A., et al., Synthesis, Structure, and Carbon Dioxide Capture Properties of Zeolitic Imidazolate Frameworks. *Acc. Chem. Res.*, **2010**, 43(1), 58-67.
[25] Britt, D., et al., Highly Efficient Separation of Carbon Dioxide by a Metal-Organic Framework Replete with Open Metal Sites. *Proc. Natl. Acad. Sci. U.S.A.*, **2009**.
[26] Banerjee, R., et al., Control of Pore Size and Functionality in Isoreticular Zeolitic Imidazolate Frameworks and Their Carbon Dioxide Selective Capture Properties. *J. Am. Chem. Soc.*, **2009**, 131(11), 3875-3877.
[27] Keskin, S., T.M. van Heest, and D.S. Sholl, Can Metal-Organic Framework Materials Play a Useful Role in Large-Scale Carbon Dioxide Separations? *ChemSusChem*, **2010**, 3(8), 879-891.
[28] Keskin, S. and D.S. Sholl, Selecting Metal Organic Frameworks as Enabling Materials in Mixed Matrix Membranes for High Efficiency Natural Gas Purification. *Energy Environ. Sci.*, **2010**, 3 343-351.
[29] Li, Y.S., et al., Controllable Synthesis of Metal-Organic Frameworks: From MOF Nanorods to Oriented MOF Membranes. *Adv. Mater.*, **2010**, 22(30), 3322-+.
[30] Zacher, D., et al., Thin Films of Metal-Organic Frameworks. *Chem. Soc. Rev.*, **2009**, 38(5), 1418-1429.
[31] Yao, J.F. and H.T. Wang, Zeolitic Imidazolate Framework Composite Membranes and Thin Films: Synthesis and Applications. *Chem. Soc. Rev.*, **2014**, 43(13), 4470-4493.
[32] Hermes, S., et al., Selective nucleation and growth of metal− organic open framework thin films on patterned COOH/CF3-terminated self-assembled monolayers on Au (111). *J. Am. Chem. Soc.*, **2005**, 127(40), 13744-13745.
[33] Liu, Y., et al., Synthesis of Continuous MOF-5 Membranes on Porous α-alumina Substrates. *Microporous Mesoporous Mater.*, **2009**, 118(1–3), 296-301.
[34] Yoo, Y., Z. Lai, and H.-K. Jeong, Fabrication of MOF-5 Membranes Using Microwave-Induced Rapid Seeding and Solvothermal Secondary Growth. *Microporous Mesoporous Mater.*, **2009**, 123(1–3), 100-106.

[35] Guo, H., et al., "Twin Copper Source" Growth of Metal-Organic Framework Membrane: $CU_3(BTC)_2$ with High Permeability and Selectivity for Recycling H_2. *J. Am. Chem. Soc.*, **2009**, 131(5), 1646-1647.

[36] Bux, H., et al., Zeolitic Imidazolate Framework Membrane with Molecular Sieving Properties by Microwave-Assisted Solvothermal Synthesis. *J. Am. Chem. Soc.*, **2009**, 131(44), 16000-16001.

[37] Huang, A., W. Dou, and J. Caro, Steam-Stable Zeolitic Imidazolate Framework ZIF-90 Membrane with Hydrogen Selectivity through Covalent Functionalization. *J. Am. Chem. Soc.*, **2010**, 132(44), 15562-15564.

[38] Wu, D., et al., Revealing The Structure-Property Relationships of Metal-Organic Frameworks for CO_2 Capture from Flue Gas. *Langmuir*, **2012**, 28(33), 12094-12099.

[39] Haldoupis, E., S. Nair, and D.S. Sholl, Finding MOFs for Highly Selective CO_2/N_2 Adsorption Using Materials Screening Based on Efficient Assignment of Atomic Point Charges. *J. Am. Chem. Soc.*, **2012**, 134(9), 4313-4323.

[40] Qiao, Z.W., K. Zhang, and J.W. Jiang, In Silico Screening of 4764 Computation-Ready, Experimental Metal-Organic Frameworks for CO_2 Separation. *J. Mater. Chem. A*, **2016**, 4(6), 2105-2114.

[41] Altintas, C., et al., A Database for CO_2 Separation Performances of MOFs Based on Computational Materials Screening. *ACS Appl. Mater. Interfaces*, **2018**.

[42] C., A., et al., Computer Simulations of 4240 MOF Membranes for H_2/CH_4 Separations: Insights into Structure–Performance Relations. *J. Mater. Chem. A*, **2018**, 6, 5836-5847.

[43] Keskin, S. and D.S. Sholl, Assessment of A Metal-Organic Framework Membrane for Gas Separations Using Atomically Detailed Calculations: CO_2, CH_4, N_2, H_2 Mixtures in MOF-5. *Ind. Eng. Chem. Res.*, **2009**, 48(2), 914-922.

[44] Cabrales-Navarro, F.A., J.L. Gómez-Ballesteros, and P.B. Balbuena, Molecular Dynamics Simulations of Metal-Organic Frameworks as Membranes for Gas Mixtures Separation. *J. Membr. Sci.*, **2013**, 428, 241-250.

[45] Krishna, R. and J.M. van Baten, In Silico Screening of Metal Organic Frameworks in Separation Applications. *Phys. Chem. Chem. Phys.*, **2011**.

[46] Battisti, A., S. Taioli, and G. Garberoglio, Zeolitic Imidazolate Frameworks for Separation of Binary Mixtures of CO_2, CH_4, N_2 and H_2: A Computer Simulation Investigation. *Microporous Mesoporous Mater.*, **2011**, 143(1), 46-53.

[47] Li, Z., et al., Molecular Simulation Studies of Flue Gas Purification by Bio-MOF. *Energies*, **2015**, 8(10), 11531-11545.

[48] Sumer, Z. and S. Keskin, Ranking of MOF Adsorbents for CO_2 Separations: A Molecular Simulation Study. *Ind. Eng. Chem. Res.*, **2016**, 55(39), 10404-10419.

[49] Yilmaz, G. and S. Keskin, Molecular Modeling of MOF and ZIF-Filled MMMs for CO_2/N_2 Separations. *J. Membr. Sci.*, **2014**, 454, 407-417.

[50] Watanabe, T. and D.S. Sholl, Accelerating Applications of Metal-Organic frameworks for Gas Adsorption and Separation by Computational Screening of Materials. *Langmuir*, **2012**, 28(40), 14114-14128.

[51] Liang, C.Z., T.-S. Chung, and J.-Y.J.P.i.P.S. Lai, A review of polymeric composite membranes for gas separation and energy production. **2019**.

[52] Powell, C.E. and G.G. Qiao, Polymeric CO_2/N_2 gas separation membranes for the capture of carbon dioxide from power plant flue gases. *J. Membr. Sci.*, **2006**, 279(1-2), 1-49.

[53] Car, A., C. Stropnik, and K.-V. Peinemann, Hybrid membrane materials with different metal–organic frameworks (MOFs) for gas separation. *Desalination*, **2006**, 200(1-3), 424-426.

[54] Basu, S., A. Cano-Odena, and I.F. Vankelecom, Asymmetric Matrimid®/[Cu3 (BTC) 2] mixed-matrix membranes for gas separations. *J. Membr. Sci.*, **2010**, 362(1-2), 478-487.

[55] Duan, C., et al., Enhanced gas separation properties of metal organic frameworks/polyetherimide mixed matrix membranes. *J. Applied Polym. Sci.*, **2014**, 131(17).

[56] Kim, J., et al., Matrix effect of mixed-matrix membrane containing CO_2 selective MOFs. *J. Applied Polym. Sci.*, **2016**, 133(1).

[57] Sumer, Z. and S. Keskin, Computational Screening of MOF-Based Mixed Matrix Membranes for CO2/N2 Separations. *J. Nanomater.*, **2016**, 2016.

[58] Erucar, I. and S. Keskin, Screening metal–organic framework-based mixed-matrix membranes for CO2/CH4 separations. *Ind. Eng. Chem. Res.*, **2011**, 50(22), 12606-12616.

[59] Chung, Y.G., et al., Computation-ready, experimental metal–organic frameworks: A tool to enable high-throughput screening of nanoporous crystals. *Chem. Mater.*, **2014**, 26(21), 6185-6192.

[60] Moghadam, P.Z., et al., Development of a Cambridge Structural Database subset: a collection of metal–organic frameworks for past, present, and future. *Chem. Mater.*, **2017**, 29(7), 2618-2625.

[61] Altintas, C. and S. Keskin, Molecular Simulations of MOF Membranes and Performance Predictions of MOF/Polymer Mixed Matrix Membranes for CO_2/CH_4 Separations. *ACS Sustainable Chem. Eng.*, **2018**, 7(2), 2739-2750.

[62] Nemati Vesali Azar, A., S. Velioglu, and S. Keskin, Large-scale Computational Screening of MOF Membranes and MOF-based Polymer Membranes for H_2/N_2 Separations. *ACS Sustainable Chem. Eng.*, **2019**, 7(10), 9525-9536.

[63] Budhathoki, S., et al., High-throughput computational prediction of the cost of carbon capture using mixed matrix membranes. *Energy Environ. Sci.*, **2019**, 12, 1255-1264.

[64] Yan, T., et al., Screening and Design of Covalent Organic Framework Membranes for CO_2/CH_4 Separation. *ACS Sustainable Chem. Eng.*, **2018**, 7(1), 1220-1227.

[65] Moghadam, P.Z., et al., Development of a Cambridge Structural Database Subset: A Collection of Metal-Organic Frameworks for Past, Present, and Future. *Chem. Mater.*, **2017**, 29(7), 2618-2625.

[66] Willems, T.F., et al., Algorithms and Tools for High-Throughput Geometry-Based Analysis of Crystalline Porous Materials. *Microporous Mesoporous Mater.*, **2012**, 149(1), 134-141.
[67] Venna, S.R., et al., Fabrication of MMMs with improved gas separation properties using externally-functionalized MOF particles. *J. Mater. Chem. A*, **2015**, 3(9), 5014-5022.
[68] Dai, Y., et al., Ultem®/ZIF-8 mixed matrix hollow fiber membranes for CO_2/N_2 separations. *J. Membrane Sci.*, **2012**, 401, 76-82.
[69] Rodrigues, M.A., et al., Nanostructured membranes containing UiO-66 (Zr) and MIL-101 (Cr) for O2/N2 and CO2/N2 separation. *Sep. Purif. Technol.*, **2018**, 192, 491-500.
[70] Meshkat, S., S. Kaliaguine, and D. Rodrigue, Mixed matrix membranes based on amine and non-amine MIL-53 (Al) in Pebax® MH-1657 for CO_2 separation. *Sep. Purif. Technol.*, **2018**, 200, 177-190.
[71] Abedini, R., A. Mosayebi, and M. Mokhtari, Improved CO2 separation of azide cross-linked PMP mixed matrix membrane embedded by nano-CuBTC metal organic framework. *Process Saf. Environ. Prot.* , **2018**, 114, 229-239.
[72] Orme, C.J., et al., Characterization of gas transport in selected rubbery amorphous polyphosphazene membranes. *J. Membrane Sci.*, **2001**, 186(2), 249-256.
[73] Sabetghadam, A., et al., Influence of Filler Pore Structure and Polymer on the Performance of MOF-Based Mixed-Matrix Membranes for CO_2 Capture. *Chem. Eur. J.*, **2018**, 24(31), 7949-7956.
[74] Lin, W.-H. and T.-S. Chung, Gas permeability, diffusivity, solubility, and aging characteristics of 6FDA-durene polyimide membranes. *J. Membrane Sci.*, **2001**, 186(2), 183-193.
[75] Budd, P.M., et al., Gas separation membranes from polymers of intrinsic microporosity. *J. Membrane Sci.*, **2005**, 251(1-2), 263-269.
[76] Merkel, T., et al., Gas sorption, diffusion, and permeation in poly (dimethylsiloxane). *J. Polym. Sci. B*, **2000**, 38(3), 415-434.
[77] Senthilkumar, U. and B. Reddy, Polysiloxanes with pendent bulky groups having amino-hydroxy functionality: structure–permeability correlation. *J. Membrane Sci.*, **2007**, 292(1-2), 72-79.
[78] Bengtson, G., S. Neumann, and V. Filiz, Membranes of polymers of intrinsic microporosity (PIM-1) modified by poly (ethylene glycol). *Membranes*, **2017**, 7(2), 28.
[79] Mizumoto, T., T. Masuda, and T. Higashimura, Polymerization of [o-(trimethylgermyl) phenyl] acetylene and polymer characterization. *J. Polym. Sci. A*, **1993**, 31(10), 2555-2561.
[80] Rappé, A.K., et al., UFF, a full periodic table force field for molecular mechanics and molecular dynamics simulations. *J. Am. Chem. Soc.*, **1992**, 114(25), 10024-10035.
[81] Mayo, S.L., B.D. Olafson, and W.A. Goddard, DREIDING: a generic force field for molecular simulations. *J. Phys. Chem.* , **1990**, 94(26), 8897-8909.
[82] Dokur, D. and S. Keskin, Effects of Force Field Selection on the Computational Ranking of MOFs for CO2 Separations. *J. Ind. eng. chem. research*, **2018**, 57(6), 2298-2309.

[83] Potoff, J.J. and J.I. Siepmann, Vapor–Liquid Equilibria of Mixtures Containing Alkanes, Carbon Dioxide, and Nitrogen. *AlChE J.*, **2001**, 47(7), 1676-1682.
[84] Makrodimitris, K., G.K. Papadopoulos, and D.N. Theodorou, Prediction of Permeation Properties of CO_2 and N_2 Through Silicalite via Molecular Simulations. *J. Phys. Chem. B*, **2001**, 105(4), 777-788.
[85] Jorgensen, W.L., et al., Comparison of Simple Potential Functions for Simulating Liquid Water. *J. Chem. Phys.*, **1983**, 79(2), 926-935.
[86] Wilmer, C.E. and R.Q. Snurr, Towards Rapid Computational Screening of Metal-Organic Frameworks for Carbon Dioxide Capture: Calculation of Framework Charges via Charge Equilibration. *Chem. Eng. J.*, **2011**, 171(3), 775-781.
[87] Dubbeldam, D., et al., RASPA: molecular simulation software for adsorption and diffusion in flexible nanoporous materials. *Mol. Simul.*, **2016**, 42(2), 81-101.
[88] Ewald, P.P., Die Berechnung Optischer und Elektrostatischer Gitterpotentiale. *Ann. Phys.*, **1921**, 369(3), 253–287
[89] Ozturk, T.N. and S. Keskin, Computational Screening of Porous Coordination Networks for Adsorption and Membrane-Based Gas Separations. *J. Phys. Chem. C*, **2014**, 118(25), 13988-13997.
[90] Vega, C., J. Abascal, and I. Nezbeda, Vapor-Liquid Equilibria from The Triple Point Up to The Critical Point for The New Generation of TIP4P-Like Models: TIP4P/Ew, TIP4P/2005, and TIP4P/Ice. *J. Chem. Phys.*, **2006**, 125(3), 034503.
[91] Frenkel, D. and B. Smit, *Understanding Molecular Simulation: From Algorithms to Applications*. 2nd ed. 2002, San Diego: Academic Press.
[92] Keskin, S. and D.S. Sholl, Efficient methods for screening of metal organic framework membranes for gas separations using atomically detailed models. *Langmuir*, **2009**, 25(19), 11786-11795.
[93] Vu, D.Q., W.J. Koros, and S. Miller, Mixed matrix membranes using carbon molecular sieves: II. Modeling permeation behavior. *J. Membrane Sci.*, **2003**, 211(2), 335-348.
[94] Moore, T.T., et al., Hybrid membrane materials comprising organic polymers with rigid dispersed phases. *AlChE J.*, **2004**, 50(2), 311-321.
[95] Shimekit, B., H. Mukhtar, and T. Murugesan, Prediction of the relative permeability of gases in mixed matrix membranes. *J. Membrane Sci.*, **2011**, 373(1-2), 152-159.
[96] Pal, R., Permeation models for mixed matrix membranes. *J. Colloid Interface Sci.* , **2008**, 317(1), 191-198.
[97] Yilmaz, G. and S. Keskin, Molecular modeling of MOF and ZIF-filled MMMs for CO2/N2 separations. *J. Membrane Sci.*, **2014**, 454, 407-417.
[98] Allen, F.H., The Cambridge Structural Database: A Quarter of a Million Crystal Structures and Rising. *Acta Crystallogr. Sect. B: Struct. Sci*, **2002**, 58(3), 380-388.
[99] Robeson, L.M., The Upper Bound Revisited. *J. Membr. Sci.*, **2008**, 320, 390–400.
[100] Bae, Y.S., et al., Enhancement of CO_2/N_2 Selectivity in A Metal-Organic Framework by Cavity Modification. *J .Mater. Chem.*, **2009**, 19(15), 2131-2134.

[101] Sholl, D.S., Understanding Macroscopic Diffusion of Adsorbed Molecules in Crystalline Nanoporous Materials via Atomistic Simulations. *Acc. Chem. Res.*, **2006**, 39(6), 403-411.
[102] Keskin, S., et al., Testing The Accuracy of Correlations for Multi-Component Mass Transport of Adsorbed Gases in Metal Organic Frameworks: Diffusion of H_2/CH_4 Mixtures in CU-BTC. *Langmuir*, **2008**, 24(15), 8254–8261.
[103] Kusakabe, K., et al., Formation of a Y-Type Zeolite Membrane on a Porous α-alumina Tube for Gas Separation. *Ind. Eng. Chem. Res.*, **1997**, 36(3), 649-655.
[104] Guo, H., et al., Hierarchical Growth of Large-Scale Ordered Zeolite Silicalite-1 Membranes with High Permeability and Selectivity for Recycling CO_2. *Angew. Chem. Int. Ed.*, **2006**, 118(42), 7211-7214.
[105] Li, S. and C.Q. Fan, High-Flux SAPO-34 Membrane for CO_2/N_2 Separation. *Ind. Eng. Chem. Res.*, **2010**, 49(9), 4399-4404.
[106] Yu, J., Y. Ma, and P.B. Balbuena, Evaluation of The Impact of H_2O, O_2, And SO_2 on Postcombustion CO_2 Capture In Metal–Organic Frameworks. *Langmuir*, **2012**, 28(21), 8064-8071.
[107] Liu, J., et al., CO_2/H_2O Adsorption Equilibrium and Rates on Metal−Organic Frameworks: HKUST-1 and Ni/DOBDC. *Langmuir*, **2010**, 26(17), 14301-14307.
[108] Burtch, N.C., H. Jasuja, and K.S. Walton, Water stability and adsorption in metal–organic frameworks. *Chem. Rev.*, **2014**, 114(20), 10575-10612.
[109] Qiao, Z., K. Zhang, and J. Jiang, In silico screening of 4764 computation-ready, experimental metal–organic frameworks for CO_2 separation. *J. Mater. Chem. A*, **2016**, 4(6), 2105-2114.
[110] Basu, S., A. Cano-Odena, and I.F. Vankelecom, MOF-containing mixed-matrix membranes for CO2/CH4 and CO2/N2 binary gas mixture separations. *Sep. Purif. Technol.*, **2011**, 81(1), 31-40.
[111] Etxeberria-Benavides, M., et al., High performance mixed matrix membranes (MMMs) composed of ZIF-94 filler and 6FDA-DAM polymer. *J. Membrane Sci.*, **2018**, 550, 198-207.
[112] Lasseuguette, E., M.-C. Ferrari, and S. Brandani, Humidity impact on the gas permeability of PIM-1 membrane for post-combustion application. *Energy Procedia*, **2014**, 63, 194-201.
[113] Sekizkardes, A.K., et al., Separation of carbon dioxide from flue gas by mixed matrix membranes using dual phase microporous polymeric constituents. *Chem. Comm.*, **2016**, 52(79), 11768-11771.
[114] Semino, R., et al., Microscopic model of the metal–organic framework/polymer interface: a first step toward understanding the compatibility in mixed matrix membranes. *ACS Appl. Mater. Interfaces*, **2015**, 8(1), 809-819.
[115] Benzaqui, M., et al., Toward an understanding of the microstructure and interfacial properties of PIMs/ZIF-8 mixed matrix membranes. *ACS Appl. Mater. Interfaces*, **2016**, 8(40), 27311-27321.

[116] Semino, R., et al., Understanding the origins of metal–organic framework/polymer compatibility. *Chem. Sci.*, **2018**, 9(2), 315-324.
[117] Huang, J., J. Zou, and W.W. Ho, Carbon dioxide capture using a CO2-selective facilitated transport membrane. *Ind. Eng. Chem. Res.*, **2008**, 47(4), 1261-1267.
[118] Erucar, I. and S. Keskin, Computational Assessment of MOF Membranes for CH_4/H_2 Separations. *J. Membr. Sci.*, **2016**, 514, 313-321.
[119] Manz, T.A. and D.S. Sholl, Chemically Meaningful Atomic Charges that Reproduce The Electrostatic Potential in Periodic and Nonperiodic Materials. *J. Chem. Theory Comput.*, **2010**, 6, 2455-2468.
[120] Zhang, L., Z. Hu, and J. Jiang, Metal–organic framework/polymer mixed-matrix membranes for H_2/CO_2 separation: a fully atomistic simulation study. *J. Phys. Chem. C*, **2012**, 116(36), 19268-19277.
[121] Semino, R., et al., Microscopic model of the metal–organic framework/polymer interface: a first step toward understanding the compatibility in mixed matrix membranes. *ACS Appl. Mater. Interfaces*, **2015**, 8(1), 809-819.
[122] Sholl, D.S. and R.P. Lively, Defects in metal–organic frameworks: challenge or opportunity? *J. Phys. Chem. Lett.*, **2015**, 6(17), 3437-3444.
[123] Zhang, Y., et al., Constructing free standing metal organic framework MIL-53 membrane based on anodized aluminum oxide precursor. **2014**, 4, 4947.
[124] Lee, D.-J., et al., Preparation of Ni-MOF-74 membrane for CO_2 separation by layer-by-layer seeding technique. **2012**, 163, 169-177.
[125] Huang, A., et al., A highly permeable and selective zeolitic imidazolate framework ZIF-95 membrane for H_2/CO_2 separation. **2012**, 48(89), 10981-10983.
[126] Liu, Y., et al., Synthesis of highly c-oriented ZIF-69 membranes by secondary growth and their gas permeation properties. *J. Membr. Sci.*, **2011**, 379(1-2), 46-51.
[127] Khdhayyer, M.R., et al., Mixed matrix membranes based on UiO-66 MOFs in the polymer of intrinsic microporosity PIM-1. *Sep. Purif. Technol.*, **2017**, 173, 304-313.
[128] Prasetya, N., B.C. Donose, and B.P.J.J.o.M.C.A. Ladewig, A new and highly robust light-responsive Azo-UiO-66 for highly selective and low energy post-combustion CO_2 capture and its application in a mixed matrix membrane for CO_2/N_2 separation. **2018**, 6(34), 16390-16402.
[129] Ren, H., et al., Affinity between metal–organic frameworks and polyimides in asymmetric mixed matrix membranes for gas separations. **2012**, 51(30), 10156-10164.

APPENDIX A: Supplementary Information for Chapter 4 and 5[§]

Table A.1. Single-component gas permeability and selectivity of polymers.

Polymer	$P^P_{CO_2}$ (Barrer)	$P^P_{N_2}$ (Barrer)	$S^P_{CO_2/N_2}$	Ref.
Matrimid	8.5	0.29	29	[67]
Ultem	1.4	0.06	25	[68]
PU	38.4	0.98	39.2	[69]
Pebax	54.4	1.7	32	[70]
PMP	76.1	3.7	20.5	[71]
MEEP	250	4	62.5	[72]
6FDA- DAM	550	38	14.5	[111]
6FDA-durene	678	38.8	17.5	[74]
PIM-7	1100	42	26.2	[75]
modified PDMS	2050.4	60	34.2	[77]
PDMS	3800	400	9.5	[76]
PIM-1	4700	243.5	19.3	[113]
PTMGP	14000	1000	14	[79]
PTMSP	29000	2700	10.74	[79]

Table A.2. Mixture permeability and selectivity of polymers.

Polymer	Pressure (bar)	Temperature (K)	$P^P_{CO_2}$ (Barrer)	$P^P_{N_2}$ (Barrer)	$S^P_{CO_2/N_2}$	Ref.
Pebax	2	298	44	0.7	62.9	[73]
Matrimid	10	308	550.3	32.4	17	[110]
PIM-1	1.25	303	7500	395	19	[112]
6FDA-DAM	1	298	780	30	26	[111]

[§] The supplementary information about MOF and MOF/Polymer MMM membranes given in this chapter was published in Journal Physical Chemistry C and Advanced Theory & Simulations with following references: Daglar, H..; Keskin, S., *Computational Screening of Metal–Organic Frameworks for Membrane-Based $CO_2/N_2/H_2O$ Separations: Best Materials for Flue Gas Separation.* Journal of Physical Chemistry C. **2018**, *122* (30), 17347–17357.; Daglar, H..; Keskin, S., *High-throughput Screening of MOFs as Fillers in Mixed Matrix Membranes for Flue Gas Separation.* Adv. Theory & Simul., 2019. This chapter is the reformatted version of the mentioned research papers.

Table A.3. Permeability measurement conditions of MOF membranes.

MOF membrane	Measured gas permeances	P (bar)	T (K)	Membrane thickness (μm)	Reference
IRMOF-1	CO_2, N_2	1.06	298	25	[33]
MIL-53 (Al)	CO_2, N_2	0.7	298	60	[123]
Ni-MOF 74	CO_2, N_2	1	298	25	[124]
ZIF-90	CO_2, N_2	1	475	20	[37]
ZIF-95	CO_2, N_2	1	600	30	[125]
ZIF-69	CO_2/N_2: 50/50	1	298	40	[126]

Table A.4. Experimental gas permeability data of MOF-based MMMs shown in Figure 5.1.

MMM	Gases	Volume Fraction (%)	Pressure (bar)	Temperature (K)	Ref.
MIL-53(Al)/Pebax	CO_2, N_2	6.0	10	308	[70]
		12.0			
		17.3			
		23.0			
UiO-66/PIM-1	CO_2, N_2	8.9	1	298	[127]
		16.4			
		22.8			
		28.3			
MIL-69(Al)/ Pebax	CO_2	20.9	1	295	[73]
MIL-69(Al)/6FDA-DAM	CO_2	23.8	1	295	[73]
UiO-66-NH_2 /PIM-1	CO_2, N_2	4.6	1	298	[127]
		8.4			
Cu-BTC/PMP	CO_2, N_2	4.7	2	303	[71]
		9.5			
		14.3			
		19.1			
UiO-66/Matrimid	CO_2, N_2	10.0	4	310	[128]
UiO-66/PU	CO_2, N_2	42.0	4	298	[69]
ZIF-71/PIM-1	CO_2, N_2	10.4	3.5	308	[129]
		20.7			
		31.0			
MIL-53(Al)/PI	CO_2, N_2	7.3	6	298	[110]
MIL-69(Al)/Pebax	CO_2/N_2: 15/85	20.9	2	298	[73]
MIL-69(Al)/6FDA-DAM	CO_2/N_2: 15/85	23.8	2	298	[73]
MIL-53(Al)/Matrimid	CO_2/N_2: 35/65	12.6	10	308	[110]
		24.5			
		35.8			

Table A.5. The refcodes of top 50 MOF fillers.

ATIBAG	DAKZEW	JIXWUJ01	NIKZEN02	VAGTUU
ATIBOU	DEBGUO	JOQSIT	OGAJEN	VAHTOQ
AWAWUQ	FIQSAA	KEPMUQ05	PUQYAC	VORZEJ
BEBYIT	GIFLEP	KEPNAX01	RATCUL03	WUZBAV
BOZGII	GUPBOJ01	KEPNAX04	RIYWIH	XEFKIC
CANVOF	HAYQIK	KEPNAX06	SEHSAC	XEGSIO
CAQFIM	IHIMAP01	LIBJUD	TIVXOM	XEGVOX
CAXRUQ	IJOMOJ06	MIXKIO	TUMBIO	YANBAR
CEWDUF	JAWGIA	MUMZAX	UHELAU	YANBAR02
DACZUF	JIXWUJ	NADFUU	UNABIW	YECTUW

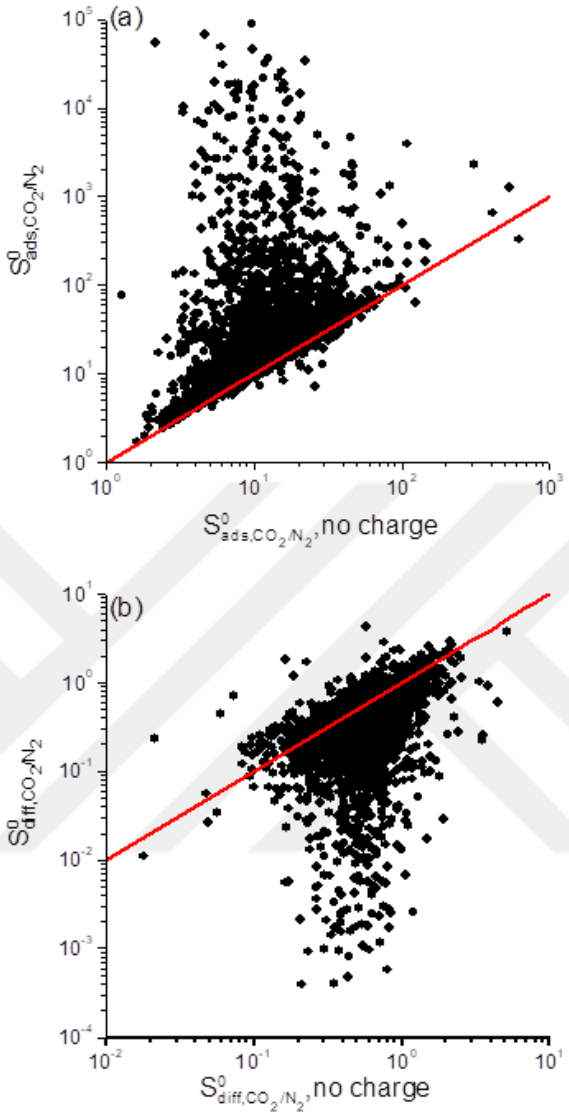

Figure A.1. Comparison of (a) adsorption and (b) diffusion selectivities of all MOFs computed with and without charge at infinite dilution, 298 K.

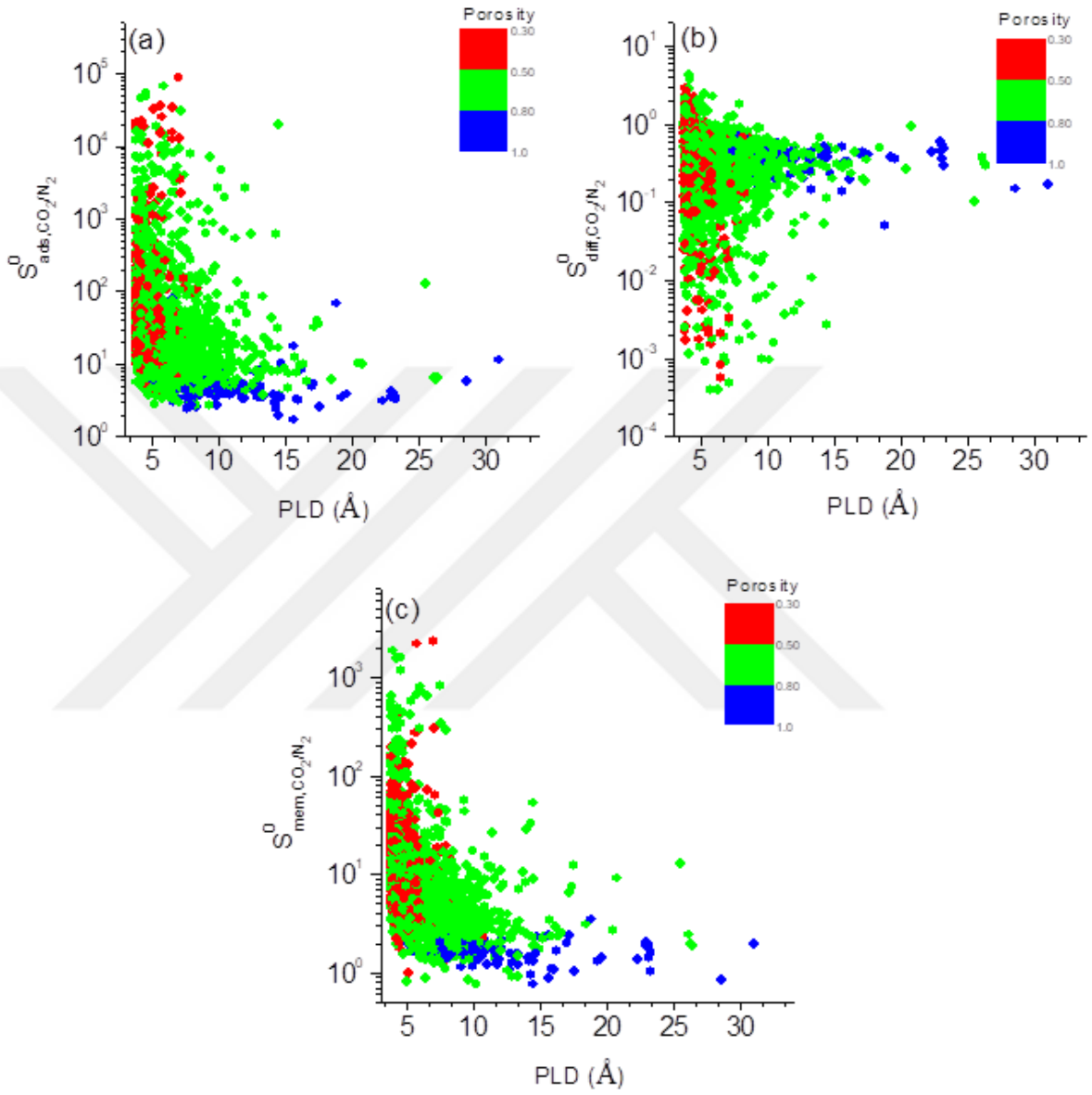

Figure A.2. (a) Adsorption selectivities, (b) diffusion selectivities, (c) membrane selectivities of all MOFs computed at infinite dilution as a function of pore limiting diameter and porosity.

VITA

Hilal Dağlar was born in Istanbul, Turkey, on 1 January 1995. In 2017, she graduated from Chemical Engineering Department on Istanbul Technical University. She successfully got her MSc degree from Chemical and Engineering Department at Koç University. Her research interests include molecular modelling of metal organic framework and theoretical calculations of mixed matrix membranes for gas separations. She is going to continue her PhD study in Chemical and Biological Engineering Department in Koç University.

Publications :

- ✓ **Daglar, H.** and S. Keskin, *High-throughput Screening of MOFs as Fillers in Mixed Matrix Membranes for Flue Gas Separation.* Adv. Theory & Simul., 2019. (This paper has been just accepted on July 22, **2019**)
- ✓ Altintas C., Avci G., **Daglar H.,** Azar A., Erucar I., Velioglu S. and Keskin S. *An Extensive Comparative Analysis of Two MOF Databases: High-Throughput Screening of Computation-Ready MOFs for CH_4 and H_2 Adsorption*. Journal of Materials Chemistry A, **2019**, 7, 9593-9608.
- ✓ **Daglar, H.** and S. Keskin, *Computational Screening of Metal–Organic Frameworks for Membrane-Based $CO_2/N_2/H_2O$ Separations: Best Materials for Flue Gas Separation.* J. Phys. Chem. C, **2018**. 122(30), 17347-17357.
- ✓ Altintas C., Avci G., **Daglar H.,** Azar A., Velioglu S., Erucar I. and Keskin S. *Database for CO_2 Separation Performances of MOFs Based on Computational Materials Screening ACS Applied Materials & Interfaces*, **2018**,10 (20), 17257-17268.
- ✓ Altintas C., Avci G., **Daglar H.,** Gulcay E., Erucar I. and Keskin S. *Computer Simulations of 4,240 MOF Membranes for H_2/CH_4 Separations: Insights into Structure-Performance Relations*, Journal of Materials Chemistry A, **2018**, 6, 5836-5847.